energies

MDPI

Article

Simultaneous Optimization of Work and Heat Exchange Networks

Nidret Ibrić [1,2,*], Chao Fu [3] and Truls Gundersen [1]

[1] Department of Energy and Process Engineering, Norwegian University of Science and Technology (NTNU), Kolbjørn Hejes v 1B, NO-7034 Trondheim, Norway; truls.gundersen@ntnu.no
[2] Faculty of Technology, University of Tuzla, Urfeta Vejzagića 8, 75000 Tuzla, Bosnia and Herzegovina
[3] SINTEF Energy Research, Sem Sælands vei 11, NO-7034 Trondheim, Norway; chao.fu@sintef.no
* Correspondence: nidret.ibric@ntnu.no or nidret.ibric@untz.ba

Abstract: This paper introduces a simultaneous optimization approach to synthesizing work and heat exchange networks (WHENs). The proposed work and heat integration (WHI) superstructure enables different thermodynamic paths of pressure and temperature-changing streams. The superstructure is connected to a heat exchanger network (HEN) superstructure, enabling the heat integration of hot and cold streams identified within the WHI superstructure. A two-step solution strategy is proposed, consisting of initialization and design steps. In the first step, a thermodynamic path model based on the WHI superstructure is combined with a model for simultaneous optimization and heat integration. This nonlinear programming (NLP) model aims to minimize operating expenditures and provide an initial solution for the second optimization step. In addition, hot and cold streams are identified, enabling additional model reduction. In the second step of the proposed solution approach, a thermodynamic path model is combined with the modified HEN model to minimize the network's total annualized cost (TAC). The proposed mixed integer nonlinear programming (MINLP) model is validated by several examples, exploring the impact of the equipment costing and annualization factor on the optimal network design. The results from these case studies clearly indicate that the new synthesis approach proposed in this paper produces solutions that are consistently similar to or better than the designs presented in the literature using other methodologies.

Keywords: heat exchanger network; work and heat integration; mathematical programming; superstructure optimization; thermodynamic path

Citation: Ibrić, N.; Fu, C.; Gundersen, T. Simultaneous Optimization of Work and Heat Exchange Networks. *Energies* **2024**, *17*, 1753. https://doi.org/10.3390/en17071753

Academic Editors: Stanislav Boldyryev and Timothy Gordon Walmsley

Received: 31 January 2024
Revised: 30 March 2024
Accepted: 3 April 2024
Published: 6 April 2024

1. Introduction

A substantial amount of energy in the form of heat and work is used in the chemical and petrochemical, metals and metallurgical, pulp and paper, food processing and other industries. Therefore, particular attention has been given to energy savings in the past half century. This has become more significant as we shift to using renewable energy sources in these industries. Heat integration (HI) has been a major development in resource conservation, providing a systematic conceptual approach to finding the best energy targets that can be obtained in any given process. The combination of mathematical programming (MP) with HI has made the methodology more easily applicable to large-scale problems of HI. Heat exchanger network (HEN) synthesis has been a popular research area for more than forty-five years [1].

In the synthesis of classical HENs, assuming constant pressure, heat is recovered from hot process streams to cold process streams, whose identity is known before optimization. When the pressure of the process streams changes, the stream's identity can also change due to the increasing temperature when compressing the stream or decreasing temperature when expanding the stream. For example, a process stream identified as a cold stream that needs heating can be compressed, resulting in an increased temperature; thus, the same

stream can then become hot. A similar conclusion can be drawn for the hot stream that needs expansion. As the hot stream expands, its temperature decreases due to cooling; thus, the stream can become cold after expansion. Because work is consumed in changing the pressure of the streams, this relatively new research concept is referred to as the work and heat exchange network (WHEN). In WHENs, pressure and temperature are two equally important and related parameters. This complex relationship is described in detail by Fu et al. [2]. The authors identified the compressor/expander inlet temperature as a crucial parameter affecting the work consumed/produced and, consequently, the hot and cold utility consumption. Two main approaches are used to solve WHEN problems: pinch analysis (PA) and MP. PA is a graphical approach that uses fundamental thermodynamic insights, and MP is based on the mathematical optimization of superstructures composed of different work and heat integration opportunities. In addition, the two approaches can also be combined to solve the problem.

Aspelund et al. [3] introduced an extended traditional PA with exergy analysis called Extended Pinch Analysis and Design (ExPAnD), which relies on a set of heuristics and engineering insights. A set of heuristic rules guiding the design is proposed for different categories of streams (pressure-changing, temperature-changing or phase-changing streams). The authors use the exergy efficiency to measure the quality of the optimal design. In a series of papers, Fu and Gundersen proposed and proved a set of fundamental theorems for the integration of compressors [4] and expanders [5] in the above ambient processes that result in designs with minimum exergy consumption. Fu et al. [6] highlighted the importance of thermodynamic insights in understanding the problem and fundamental concepts, but they also presented limitations, especially when addressing the network cost. For this particular reason, the MP approach has attracted more research interest.

Wechsung et al. [7] proposed a state-space superstructure consisting of pressure-changing stages separately for hot and cold streams and a pinch operator for heat integration, capable of handling variable temperatures. However, compression and expansion are achieved at the pinch temperature according to the proposed ExPanD methodology [3], which might yield sub-optimal solutions. The objective function minimizes exergy consumption. Huang and Karimi [8] proposed a multistage superstructure with separate HEN and work exchange network (WEN) blocks within each stage. The superstructure is distinct for low-pressure streams that are compressed and high-pressure streams that are expanded. Stream splitting enables utility compression/expansion, valves and single-shaft turbine compressors (SSTCs) with the same optimized inlet temperature. The HEN superstructure is a stage-wise superstructure that includes non-isothermal mixing [9]. The objective function minimizes the total annualized cost (TAC) of the network. Onishi et al. [10] proposed a multistage work integration superstructure with heat integration between the WEN stages. The HEN model is based on the well-known stage-wise superstructure by Yee and Grossmann [11]. Streams are classified as high-pressure and low-pressure streams, for which the WEN superstructure differs. The WEN stage consists of parallel branches of turbines and compressors on a common SSTC. Turbines are associated with stages for high-pressure streams, enabling work recovery from high-pressure to low-pressure streams, with an additional utility turbine and an expansion valve. For low-pressure streams, there is an equal number of compressors corresponding to the number of turbines and utility compressors on a single shaft. Compared to the work of Huang and Karimi [8], parallel SSTC units are possible, including utility compressors and turbines. Helper motors and turbine generators exist within SSTC units to deal with an excess or shortage of energy. The streams are sent to the HEN between the WEN stages to improve the pressure recovery. The objective function minimizes the TAC of a combined HEN and WEN. However, in the work of Onishi et al. [12], the classical stage-wise superstructure for HEN synthesis [11] is intertwined with the predefined pressure change network for hot and cold streams. In this approach, the hot and cold streams follow specific pressure change routes with a maximum of three stages of expansion and compression. Unlike most MP deterministic approaches, modeled using algebraic languages such as the General Algebraic Modeling

System (GAMS), Pavão et al. [13] proposed a new meta-heuristic approach, a matrix-based implementation of a WHEN superstructure, inspired by previous works [7,14] coupled with an enhanced stage-wise HEN superstructure [15]. This work was later extended [16], including additional structural possibilities for work and heat integration with practical constraints (upper/lower bounds on temperature) for pressure change units, as well as a number of coupled units (compressors and turbines) per shaft. A framework for simultaneous WHI based on a mixed integer nonlinear programming (MINLP) model was proposed by Nair et al. [17]. In the proposed framework, the streams are unclassified, and the pressure change is also allowed for constant pressure streams. In addition, the authors considered the phase changes of streams with phase-based property calculations. In the proposed superstructure, each stream starts at a specific pressure and temperature and passes through a series of WHEN stages to reach its final pressure. A WHEN stage comprises a typical stage-wise HEN as in Huang et al. [9] and pressure change units consisting of SSTCs and valves. A similar superstructure to those proposed by Huang and Karimi [8] and Nair et al. [17] has been developed by Onishi et al. [18], with an approach combining MP with a pinch location method [19,20] to obtain an optimal network design with the minimum TAC. The authors proposed a generalized disjunctive programming (GDP) model for the selection of pressure change equipment in the work integration stages and the identification of unclassified streams. The model is also suitable for the handling of unknown inlet and outlet temperatures. Although the authors claim global optimality, Fu et al. [6] obtained better solutions with their graphical approach that minimizes the exergy consumption rather than the TAC of the network.

Li et al. [21] proposed an alternative approach to presenting all potential flowsheet configurations for WHENs with building blocks. These blocks consist of block interiors representing the mixing, splitting, utility heating/cooling and boundaries between adjacent blocks that allow for work and heat integration. Contrary to other proposed superstructures, this approach does not require work and heat integration stages and includes equipment such as two-stream and multi-stream heat exchangers, compressors/expanders and SSTCs. The model is formulated as an MINLP with the objective function of minimizing the TAC. Pavão et al. [22] used a pinch-based approach to define pressure-changing routes based on capital and operating cost targets before detailed WHEN synthesis and provided an efficient starting point for WHEN synthesis. The solution approach is a hybrid meta-heuristic method based on stochastic methods to define modifications to the pressure manipulation route. The obtained pressure-changing routes are fixed, and then the HI problem is solved with a specified heat recovery approach temperature (HRAT) using the approach of "spaghetti" design to reduce the heat transfer area [23]. Previous steps are used as an initial design for the simultaneous WHEN problem. This paper highlights the importance of targeting before the design step, while Yu et al. [24] presented alternative formulations for the simultaneous optimization and heat integration of WHENs. A two-step sequential design procedure was proposed by Lin et al. [25]. In the first step of the proposed approach, a stage-wise superstructure, in which the unclassified streams subsequently go through the HEN and WEN stages, is used to perform a targeting procedure with an extended PA method under the assumption of vertical heat transfer. When the optimal thermodynamic path is identified with the proposed GDP model, the HEN is synthesized using a stage-wise HEN superstructure and an MINLP model [11]. The solution approach was later modified [26] with an efficient optimization strategy by modifying the targeting step to identify the optimal thermodynamic paths of process streams using genetic algorithms and a golden section search. The HEN design is determined using a global search algorithm in the design phase. Lin et al. [27] presented a solution procedure to obtain globally optimal WHEN designs based on a minimal WHEN system using an enumeration procedure on predefined thermodynamic paths. In addition, the properties of the streams are calculated using cubic equations of state; however, because the authors used a reduced minimal WHEN representation to obtain simple designs, the presented solutions are not global solutions to the problem, as later shown in this paper.

Most of the previous research has been focused on minimizing the TAC of the network. Yang et al. [28] presented a multi-objective MINLP model for the synthesis of WHENs, including constant-pressure and pressure-changing streams with multi-stage compression. However, their proposed stage-wise superstructure includes only the compression of predefined cold streams. The Pareto front of the solutions has opposing objectives: minimizing the TAC and the exergy consumption. A similar superstructure was created to address the expansion of hot, high-pressure streams [29], later modified to include a simple model for the steam Rankine cycle for a utility system in order to account for multiple utilities [30]. Braccia et al. [31] combined the WHEN superstructure proposed by Huang and Karimi [8] with the HEN superstructure of Yee and Grossmann [11], enabling a change in stream identities with explicit modeling, avoiding additional binary variables and nonlinearities. This allows the pressure-changing streams to act as a low-pressure hot stream and a high-pressure cold stream at different stages in the proposed network. For a more detailed and in-depth analysis of thermodynamic-based and optimization-based methods for WHEN synthesis, the reader is referred to a recent review paper by Yu et al. [32]. The authors present a review of application studies and the equipment used in work and heat integration, as well as a critical review of the studies regarding the methods, pressure change equipment, property models and objective function.

There are several limitations in previous research on work and heat integration. The fundamental thermodynamic approach of Fu and Gundersen [4,5] only considered energy performance (exergy), neglecting the investment cost or TAC. Some optimization-based approaches [17,18] use superstructures that do not include certain topological combinations related to HEN configurations. Other methodologies have used a predefined thermodynamic path for pressure-changing streams [7,27], while some studies only consider the compression of cold streams [28] and/or the expansion of hot streams [29].

This work presents a novel WHI superstructure based on feasible thermodynamic paths involving the multi-choice mixing and splitting of streams. In the presented superstructure, the streams are unclassified but identified as hot and cold within different superstructure elements. A two-step solution strategy consisting of a targeting/initialization step and a design step is proposed. Contrary to much previous research, where the targeting is used to fix the thermodynamic paths, this work uses the targeting model for stream identification and the initialization of the MINLP model for the simultaneous synthesis of the WHEN, performed in the second step. In addition, most studies use the stage-wise superstructure [11] and its modifications to design the HEN within the WHEN. In this work, we use a modified superstructure from Floudas et al. [33] that gives additional heat integration opportunities when integrated with a WHI superstructure. Furthermore,the HRAT temperature required for the targeting step can be changed to provide different initializations and generate a set of local solutions to the MINLP model.

2. Problem Formulation

Figure 1 shows the conceptual formulation of the work and heat exchange network (WHEN) synthesis problem. Given is a set of process streams $s \in S$ with specified supply and target parameters (pressure and temperature). The process streams are connected to the heat exchanger network (HEN), consisting of heat exchangers, heaters (H) and coolers (C), enabling heat integration, and the work exchange network (WEN), consisting of compressors, expanders and expansion valves, enabling pressure changes in process streams. The HEN and WEN are interconnected, enabling the simultaneous optimization of work and heat integration. The system requires hot and cold utilities for additional heating and cooling within the HEN and electricity required/produced by running compressors and expanders.

The objective is to synthesize the optimal network design with the minimum TAC. This implies finding the optimal placement of the pressure change equipment within the HEN. The following assumptions are imposed to simplify the synthesis procedure.

- Steady-state operation is considered.

- All process streams are ideal gaseous streams.
- Compression and expansion are reversible and adiabatic (i.e., isentropic).
- Expansion through the valve is isenthalpic with a constant Joule–Thompson coefficient.
- One hot and one cold utility is assumed.
- The compressor and expander isentropic efficiency is considered constant.
- The heat capacity flow rates are constant.
- Heat and pressure losses are neglected.
- The costs of mixers and expansion valves are negligible.

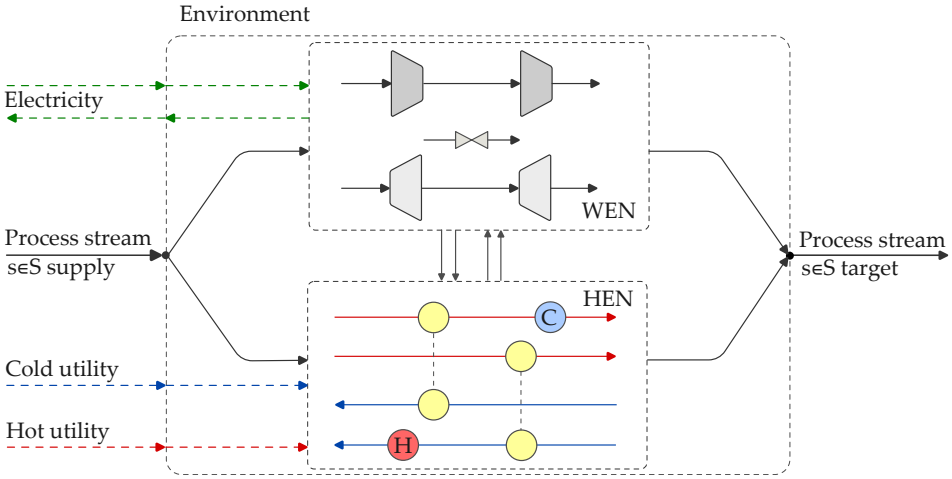

Figure 1. Conceptual problem formulation.

3. Methodology

3.1. Possible Thermodynamic Paths

To create a superstructure, we start with the feasible thermodynamic paths (trajectories) shown in Figure 2, previously studied in the literature [34] for the change in state for process streams. Let us observe a state change (1 → 2) where the stream requires compression and heating (low-pressure cold stream), assuming that the isentropic efficiency is 1 (ideal isentropic compression). The stream can be compressed from its initial state and cooled afterwards, following the path (1 → a → 2). This trajectory requires compression at higher temperatures, and more work is consumed for the compression. Still, it produces higher outlet temperatures in the stream (high-quality heat) that can be used for heat integration. An additional increase in the compressor inlet temperature creates better-quality heat (path 1 → e → f → 2). However, it may not be practical to compress the stream at higher temperatures due to limitations in the operating conditions of the compressors. To reduce the compressor inlet temperature, it is possible to cool down the compressor inlet stream (at constant pressure), followed by the compression of the stream (path 1 → b → 2). An additional decrease in the compressor inlet temperature requires additional heating after the compression of the stream (path 1 → c → d → 2). Reducing the compressor inlet temperature consumes less compression work, but the compressor outlet temperature decreases, and the quality of the heat is lower.

If we now consider that the stream is compressed to a pressure higher than required, the possible number of thermodynamic paths increases significantly. The stream can be cooled and compressed to pressure $p > p_2$ (1 → c → h) and, after this, expanded in a pressure reduction valve and cooled to the required temperature (h → a → 2). Expansion can also be done in an expander, producing the work (h → i → 2).

Similarly, the diagram shown in Figure 2 can also be used to analyze the thermodynamic paths of a high-pressure hot stream (change of state 2 → 1). The same trajectories can be followed but in the reverse direction of the pressure change. However, the expansion of the process stream has the opposite effect compared to compression. Increasing the inlet

temperature of the expander increases the work production in the expander. On the other hand, high-quality heat is not available for heat integration because it is used to produce work. The thermodynamic path (2 → a → 1) shows the expansion process ending at a specified target temperature T_1. An additional increase in the expander inlet temperature produces more work but requires the additional cooling of the stream leaving the expander (path 2 → f → e → 1). Thermodynamic path 2 → b → 1 starts with expansion at the supply state and requires additional heating to reach the target state, and thermodynamic path 2 → d → c → 1 includes cooling before expanding the stream in the expander. Expansion to the required pressure can be done by using an expansion valve (isenthalpic process); however, work is not being produced in this case, and there is a significant loss in the exergy of the stream. After the expansion, additional cooling is required (path 2 → g → 1). As can be seen, many possible thermodynamic paths exist for the change of state 1 → 2 or 2 → 1. In theory, if we assume that change of state 1 → 2 can be achieved by combining compression, expansion, cooling and heating at any feasible pressure and temperature, as long as we start at state (1) and end up at state (2), there can be an infinite number of trajectories. However, most of them would be impractical.

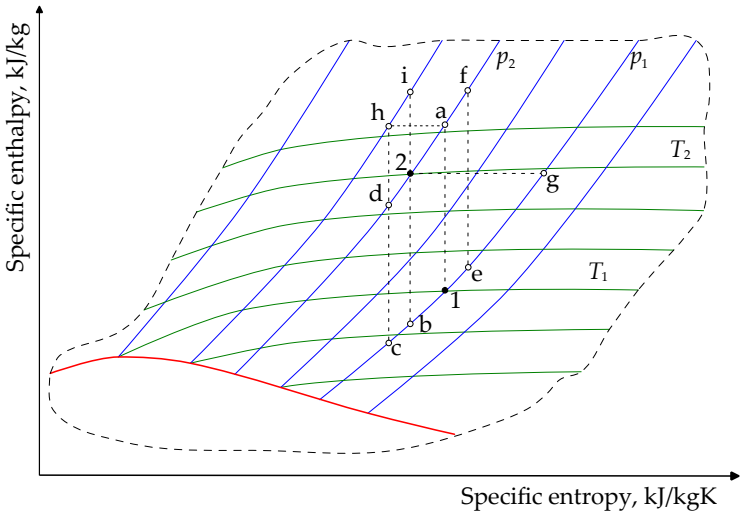

Figure 2. Hypothetical thermodynamic paths for compression and expansion of streams.

It should be noticed that the objective of the feasible thermodynamic paths stage of the method proposed by Yu et al. [34] is to fix the stream data before performing traditional HEN synthesis. In contrast, the feasible thermodynamic paths stage of the present method only serves to identify process streams and initialize the WHEN synthesis, where the process stream variables (pressure, temperature and branch flow rates) are allowed to change. This paper addresses the problem of finding the optimal trajectory for pressure-changing streams and simultaneously optimizing the HEN by minimizing the TAC of the network. We begin by synthesizing the superstructure based on the trajectories shown in Figure 2.

3.2. Work and Heat Integration (WHI) Superstructure

A superstructure shown in Figure 3 has been designed based on practical and feasible thermodynamic paths. This superstructure enables the exploration of various trajectories for stream *s* from the supply to the target state. In the proposed superstructure, the multi-choice splitting of stream *s* enables the heating or cooling of a stream before compression or expansion. We use the term multi-choice splitting because hot and cold stream branches can exist simultaneously (not a single-choice selection). It is important to highlight that the stream can remain isothermal when there is no temperature change in the heat exchangers. Multi-stage compression with inter-stage cooling enables the pressure increase of stream *s*, allowing for additional savings in the work required for compression (not shown in Fig-

ure 2). Conversely, the pressure reduction is achieved through multi-stage expansion with inter-stage heating, maximizing the work output, or with an expansion valve. The bypass option is incorporated to accommodate non-pressure-changing streams. The heating and cooling of process stream s leaving the pressure-changing stage $k = |K|$ is enabled by the multi-choice mixing of stream s, where hot and cold branches can exist simultaneously with multi-choice selection.

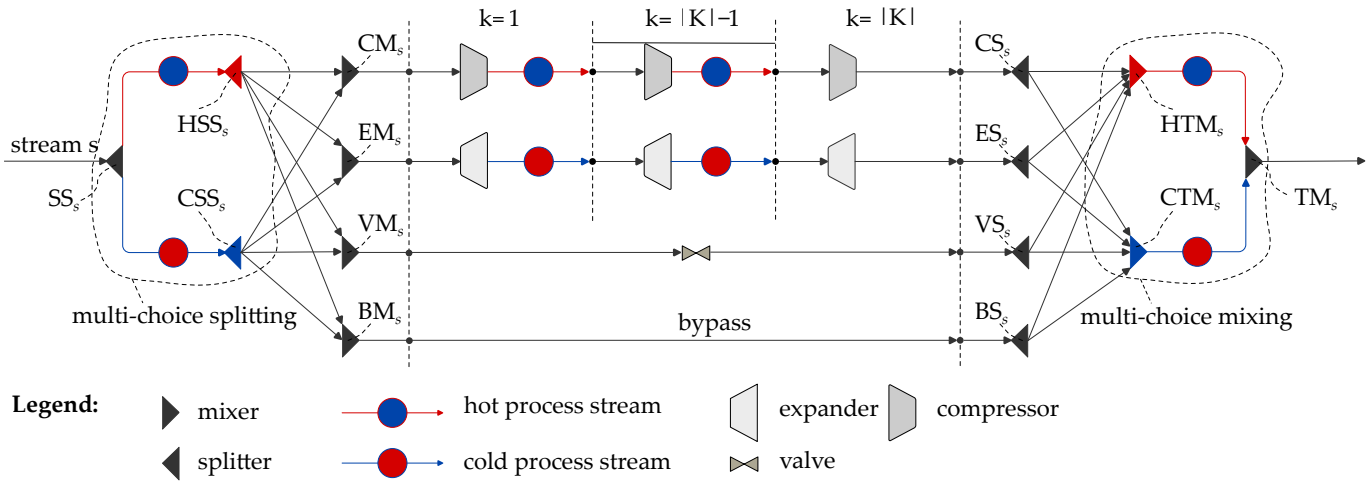

Figure 3. Work and heat integration (WHI) superstructure.

The proposed superstructure enables the heating and cooling of streams at the supply pressure, pressure change or bypass for non-pressure-changing streams, and the heating and cooling of streams at the target pressure. The proposed superstructure captures heat integration opportunities within and outside the pressure-changing stages. Additionally, it enables the search for the optimal placement of the pressure-changing equipment to minimize the network's TAC. The number of pressure-changing stages is set arbitrarily by the user.

The symbols used for the mixing and splitting units in the superstructure of Figure 3 have the following meanings:

SS_s Supply splitter for stream s;
HSS_s Supply splitter for a potential hot stream s;
CSS_s Supply splitter for a potential cold stream s;
CM_s Mixer before compressor for stream s;
EM_s Mixer before expander for stream s;
VM_s Mixer before valve for stream s;
BM_s Mixer before bypass for stream s.

The splitters CS_s, ES_s, VS_s and BS_s have similar meanings for stream s after the corresponding operation (compression, expansion, valve and bypass):

HTM_s Target mixer for a potential hot stream s;
CTM_s Target mixer for a potential cold stream s;
TM_s Target mixer for stream s.

3.3. Heat Exchanger Network (HEN) Superstructure

The HEN superstructure is based on the superstructure proposed by Floudas et al. [33], with small modifications regarding the introduction of a bypass connection for isothermal streams (Figure 4). Figure 4a shows the superstructure design for a hot stream i matched with cold streams j in exchanger $i - j$. The initial splitter S_i allows the parallel arrangement of the heat exchangers and mixers/splitters (EM_i and ES_i) in front of/behind each exchanger $i - j$, enabling the configuration of heat exchangers in series. The additional cooling of a hot stream i is possible in cooler $i - C$. The superstructure design for cold stream j matched

with hot streams i in heat exchanger $i-j$ is shown in Figure 4b. However, the HEN superstructure in Floudas et al. [33] is derived based on the previous solution of two consecutive targeting models to minimize the utility consumption and number of matches. Thus, the model is easier to solve when knowing the supply and target temperatures of all hot and cold streams within the network and the corresponding minimum number of matches (with given duties) used to design the superstructure. In contrast, when designing the WHEN superstructure, the identity and temperature of the streams can be changed due to compression and expansion, and thus the inlet–outlet temperatures are optimization variables. This makes the synthesis problem much more difficult to solve. In addition, when the HEN superstructure (Figure 4) is coupled with the WHI superstructure (Figure 3), it enables more heat integration opportunities than the standalone HEN superstructure.

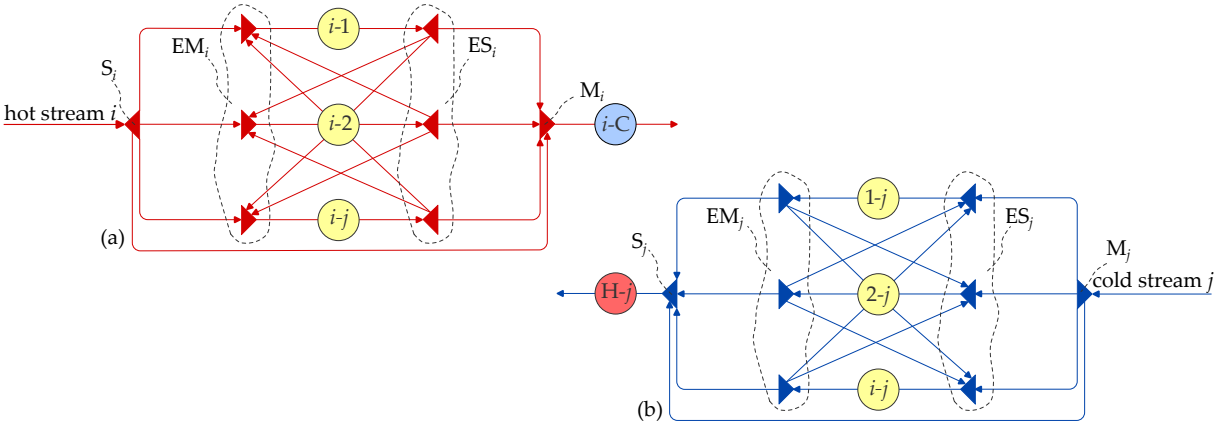

Figure 4. The HEN superstructure for (**a**) hot stream i (**b**) cold stream j.

3.4. Model

The overall model consists of three models: the thermodynamic path model (M_1), the heat integration (HI) model M_2 of Duran and Grossmann [19] and the HEN model M_3. To address the WHEN synthesis problem, the models are connected using appropriate equations to identify the streams and connect the models, as presented in Appendix A.1. A detailed description of the proposed models follows.

3.4.1. The Thermodynamic Path Model

The thermodynamic path model (M_1) is based on the WHI superstructure (Figure 3) that enables the identification of streams and the optimum placement for the pressure change equipment.

Multi-choice splitting. Stream s is unclassified, which means that it can be either hot or cold. Thus, according to Equation (1), the stream is divided in splitter SS_s into fractions of the heat capacity flow rate serving as both hot and cold streams.

$$m_s = m_s^{(\mathrm{hs})} + m_s^{(\mathrm{cs})}, \quad \forall s \in S \tag{1}$$

These split fractions of hot and cold stream s are directed to the mixers before pressure change stage $k = 1$. However, the stream cannot be of low and high pressure simultaneously. Thus, auxiliary binary parameters (CINT, EINT, BINT) are introduced with assigned values based on the supply ($p_s^{(\mathrm{in})}$) and target pressure ($p_s^{(\mathrm{out})}$). For example, if the supply pressure is lower than the target pressure ($p_s^{(\mathrm{in})} < p_s^{(\mathrm{out})}$), the stream requires compression, and thus CINT = 1, and EINT = 0 and BINT = 0 for a specified stream s. Otherwise, if $p_s^{(\mathrm{in})} > p_s^{(\mathrm{out})}$ EINT = 1, CINT = 0 and BINT = 0. In the case of of $p_s^{(\mathrm{in})} = p_s^{(\mathrm{out})}$, then BINT = 1. Equations (2)

and (3) represent the mass balance equations for the splitters of hot (HSS_s) and cold (CSS_s) supply streams.

$$m_s^{(\mathrm{hs})} = \underset{\mathrm{CINT}=1}{m_s^{(\mathrm{hs}\to\mathrm{comp})}} + \underset{\mathrm{EINT}=1}{m_s^{(\mathrm{hs}\to\mathrm{exp})}} + \underset{\mathrm{EINT}=1}{m_s^{(\mathrm{hs}\to\mathrm{valve})}} + \underset{\mathrm{BINT}=1}{m_s^{(\mathrm{hs}\to\mathrm{bypass})}}, \quad \forall s \in S \tag{2}$$

$$m_s^{(\mathrm{cs})} = \underset{\mathrm{CINT}=1}{m_s^{(\mathrm{cs}\to\mathrm{comp})}} + \underset{\mathrm{EINT}=1}{m_s^{(\mathrm{cs}\to\mathrm{exp})}} + \underset{\mathrm{EINT}=1}{m_s^{(\mathrm{cs}\to\mathrm{valve})}} + \underset{\mathrm{BINT}=1}{m_s^{(\mathrm{cs}\to\mathrm{bypass})}}, \quad \forall s \in S \tag{3}$$

Mixers in front of pressure change stages. Streams from splitters (HSS_s and CSS_s) are directed to the pressure change stages or act as bypass streams if $p_s^{(\mathrm{in})} = p_s^{(\mathrm{out})}$. Several mixers for the compressor (CM_s), expander (EM_s), valve (VM_s) and bypass stream (BM_s) can be identified in the superstructure shown in Figure 3, for which the mass and heat balances are given by Equations (4)–(11).

$$m_s^{(\mathrm{comp})} = m_s^{(\mathrm{hs}\to\mathrm{comp})} + m_s^{(\mathrm{cs}\to\mathrm{comp})}, \quad \forall s \in S, \mathrm{CINT} = 1 \tag{4}$$

$$m_s^{(\mathrm{comp})} T_s^{(\mathrm{comp,in})} = m_s^{(\mathrm{hs}\to\mathrm{comp})} T_s^{(\mathrm{hs,out})} + m_s^{(\mathrm{cs}\to\mathrm{comp})} T_s^{(\mathrm{cs,out})}, \quad \forall s \in S, \mathrm{CINT} = 1 \tag{5}$$

$$m_s^{(\mathrm{exp})} = m_s^{(\mathrm{hs}\to\mathrm{exp})} + m_s^{(\mathrm{cs}\to\mathrm{exp})}, \quad \forall s \in S, \mathrm{EINT} = 1 \tag{6}$$

$$m_s^{(\mathrm{exp})} T_s^{(\mathrm{exp,in})} = m_s^{(\mathrm{hs}\to\mathrm{exp})} T_s^{(\mathrm{hs,out})} + m_s^{(\mathrm{cs}\to\mathrm{exp})} T_s^{(\mathrm{cs,out})}, \quad \forall s \in S, \mathrm{EINT} = 1 \tag{7}$$

$$m_s^{(\mathrm{valve})} = m_s^{(\mathrm{hs}\to\mathrm{valve})} + m_s^{(\mathrm{cs}\to\mathrm{valve})}, \quad \forall s \in S, \mathrm{EINT} = 1 \tag{8}$$

$$m_s^{(\mathrm{valve})} T_s^{(\mathrm{valve,in})} = m_s^{(\mathrm{hs}\to\mathrm{valve})} T_s^{(\mathrm{hs,out})} + m_s^{(\mathrm{cs}\to\mathrm{valve})} T_s^{(\mathrm{cs,out})}, \quad \forall s \in S, \mathrm{EINT} = 1 \tag{9}$$

$$m_s^{(\mathrm{bypass})} = m_s^{(\mathrm{hs}\to\mathrm{bypass})} + m_s^{(\mathrm{cs}\to\mathrm{bypass})}, \quad \forall s \in S, \mathrm{BINT} = 1 \tag{10}$$

$$m_s^{(\mathrm{bypass})} T_s^{(\mathrm{bypass}} = m_s^{(\mathrm{hs}\to\mathrm{bypass})} T_s^{(\mathrm{hs,out})} + m_s^{(\mathrm{cs}\to\mathrm{bypass})} T_s^{(\mathrm{cs,out})}, \quad \forall s \in S, \mathrm{BINT} = 1 \tag{11}$$

Compression stages. Multi-stage compression with inter-stage cooling enables a pressure increase in the compression stages. The compression work in stage k is given by Equation (12).

$$W_{s,k}^{(\mathrm{comp})} = m_s^{(\mathrm{comp})} \left(T_{s,k}^{(\mathrm{comp,out})} - T_{s,k}^{(\mathrm{comp,in})} \right), \quad \forall s \in S, \forall k \in K, \mathrm{CINT} = 1 \tag{12}$$

The ideal temperature increase following compression is directly linked to the increase in pressure as given by Equation (13) under the assumption of isentropic compression, ideal gas, and constant specific heat capacity. The actual temperature increase accounting for the compressor's isentropic efficiency is given by Equation (14).

$$T_{\mathrm{id},s,k}^{(\mathrm{comp,out})} = T_{s,k}^{(\mathrm{comp,in})} \left(\frac{p_{s,k}^{(\mathrm{comp,out})}}{p_{s,k}^{(\mathrm{comp,in})}} \right)^{\frac{\kappa-1}{\kappa}}, \quad \forall s \in S, \forall k \in K, \mathrm{CINT} = 1 \tag{13}$$

$$T_{s,k}^{(\mathrm{comp,out})} = T_{s,k}^{(\mathrm{comp,in})} + \left(\frac{T_{\mathrm{id},s,k}^{(\mathrm{comp,out})} - T_{s,k}^{(\mathrm{comp,in})}}{\eta} \right), \quad \forall s \in S, \forall k \in K, \mathrm{CINT} = 1 \tag{14}$$

Equations (15) and (16) set the pressure and temperature constraints for each compression stage $k \in K$.

$$T_{s,k}^{(\mathrm{comp,out})} \geq T_{s,k}^{(\mathrm{comp,in})}, \quad \forall s \in S, \forall k \in K, \mathrm{CINT} = 1 \tag{15}$$

$$p_{s,k}^{(\mathrm{comp,out})} \geq p_{s,k}^{(\mathrm{comp,in})}, \quad \forall s \in S, \forall k \in K, \mathrm{CINT} = 1 \tag{16}$$

Temperature and pressure equality constraints apply for the compression stages $k \in K$ as given by Equations (17)–(23).

$$T_{s,k=1}^{(\mathrm{comp,in})} = T_s^{(\mathrm{comp,in})}, \quad \forall s \in S, \mathrm{CINT} = 1 \tag{17}$$

$$T_{s,k}^{(\text{comp,in})} = T_{s,k-1}^{(\text{IC,out})}, \quad \forall s \in S, k \neq 1, \text{CINT} = 1 \tag{18}$$

$$T_{s,k}^{(\text{comp,out})} = T_{s,k}^{(\text{IC,in})}, \quad \forall s \in S, k \neq |K|, \text{CINT} = 1 \tag{19}$$

$$T_{s,k=|K|}^{(\text{comp,out})} = T_{s}^{(\text{comp,out})}, \quad \forall s \in S, \text{CINT} = 1 \tag{20}$$

$$p_{s,k=1}^{(\text{comp,in})} = p_{s}^{(\text{in})}, \quad \forall s \in S, \text{CINT} = 1 \tag{21}$$

$$p_{s,k}^{(\text{comp,in})} = p_{s,k-1}^{(\text{comp,out})}, \quad \forall s \in S, k \neq 1, \text{CINT} = 1 \tag{22}$$

$$p_{s,k=|K|}^{(\text{comp,out})} = p_{s}^{(\text{out})}, \quad \forall s \in S, \text{CINT} = 1 \tag{23}$$

Expansion stages. Multi-stage expansion with inter-stage heating enables a pressure decrease in the stages of expansion. The expansion work in stage k is given by Equation (24).

$$W_{s,k}^{(\text{exp})} = m_{s}^{(\text{exp})} \left(T_{s,k}^{(\text{exp,in})} - T_{s,k}^{(\text{exp,out})} \right), \quad \forall s \in S, \forall k \in K, \text{EINT} = 1 \tag{24}$$

The temperature decrease following the expansion is directly linked to the decrease in pressure as given by Equation (25) under the assumption of ideal expansion. The actual temperature decrease accounting for the expander's isentropic efficiency is given by Equation (26).

$$T_{\text{id},s,k}^{(\text{exp,out})} = T_{s,k}^{(\text{exp,in})} \left(\frac{p_{s,k}^{(\text{exp,out})}}{p_{s,k}^{(\text{exp,in})}} \right)^{\frac{\kappa-1}{\kappa}}, \quad \forall s \in S, \forall k \in K, \text{EINT} = 1 \tag{25}$$

$$T_{s,k}^{(\text{exp,out})} = T_{s,k}^{(\text{exp,in})} - \eta \left(T_{s,k}^{(\text{exp,in})} - T_{\text{id},s,k}^{(\text{exp,out})} \right), \quad \forall s \in S, \forall k \in K, \text{EINT} = 1 \tag{26}$$

Equations (27) and (28) set the temperature and pressure constraints for each expansion stage $k \in K$.

$$T_{s,k}^{(\text{exp,in})} \geq T_{s,k}^{(\text{exp,out})}, \quad \forall s \in S, \forall k \in K, \text{EINT} = 1 \tag{27}$$

$$p_{s,k}^{(\text{exp,in})} \geq p_{s,k}^{(\text{exp,out})}, \quad \forall s \in S, \forall k \in K, \text{EINT} = 1 \tag{28}$$

Temperature and pressure equality constraints apply for the expansion stages $k \in K$ as given by Equations (29)–(35).

$$T_{s,k=1}^{(\text{exp,in})} = T_{s}^{(\text{exp,in})}, \quad \forall s \in S, \text{EINT} = 1 \tag{29}$$

$$T_{s,k}^{(\text{exp,in})} = T_{s,k-1}^{(\text{IH,out})}, \quad \forall s \in S, k \neq 1, \text{EINT} = 1 \tag{30}$$

$$T_{s,k}^{(\text{exp,out})} = T_{s,k}^{(\text{IH,in})}, \quad \forall s \in S, k \neq |K|, \text{EINT} = 1 \tag{31}$$

$$T_{s,k=|K|}^{(\text{exp,out})} = T_{s}^{(\text{exp,out})}, \quad \forall s \in S, \text{EINT} = 1 \tag{32}$$

$$p_{s,k=1}^{(\text{exp,in})} = p_{s}^{(\text{in})}, \quad \forall s \in S, \text{EINT} = 1 \tag{33}$$

$$p_{s,k}^{(\text{exp,in})} = p_{s,k-1}^{(\text{exp,out})}, \quad \forall s \in S, k \neq 1 \text{EINT} = 1 \tag{34}$$

$$p_{s,k=|K|}^{(\text{exp,out})} = p_{s}^{(\text{out})}, \quad \forall s \in S, \text{EINT} = 1 \tag{35}$$

Expansion valves. Pressure reduction in expansion valves is an isenthalpic process. The temperature change due to change in pressure is determined by the Joule–Thompson expansion coefficient (μ), as given by Equation (36). The sign of the Joule–Thomson

coefficient determines whether the process is characterized as cooling ($\mu < 0$) or heating ($\mu > 0$).

$$T_s^{(\text{valve,out})} = T_s^{(\text{valve,in})} + \mu\left(p_s^{(\text{valve,in})} - p_s^{(\text{valve,out})}\right), \quad \forall s \in S, \text{EINT} = 1 \tag{36}$$

Equation (37) gives an inequality constraint linked to pressure changes during expansion, while Equations (38) and (39) represent equality constraints for the supply and target pressures.

$$p_s^{(\text{valve,in})} \geq p_s^{(\text{valve,out})}, \quad \forall s \in S, \text{EINT} = 1 \tag{37}$$

$$p_s^{(\text{valve,in})} = p_s^{(in)}, \quad \forall s \in S, \text{EINT} = 1 \tag{38}$$

$$p_s^{(\text{valve,out})} = p_s^{(\text{out})}, \quad \forall s \in S, \text{EINT} = 1 \tag{39}$$

Splitters after pressure change stages. Fractions of process stream s exiting a pressure change or bypass stages are directed to a multi-choice mixer, enabling heating and cooling. The mass balance equations for the compressor (CS_s), expander (ES_s), expansion valve (VS_s) and bypass (BS_s) splitters are provided by Equations (40)–(43).

$$m_s^{(\text{comp})} = m_s^{(\text{comp}\to\text{ht})} + m_s^{(\text{comp}\to\text{ct})}, \quad \forall s \in S, \text{CINT} = 1 \tag{40}$$

$$m_s^{(\text{exp})} = m_s^{(\text{exp}\to\text{ht})} + m_s^{(\text{exp}\to\text{ct})}, \quad \forall s \in S, \text{EINT} = 1 \tag{41}$$

$$m_s^{(\text{valve})} = m_s^{(\text{valve}\to\text{ht})} + m_s^{(\text{valve}\to\text{ct})}, \quad \forall s \in S, \text{EINT} = 1 \tag{42}$$

$$m_s^{(\text{bypass})} = m_s^{(\text{bypass}\to\text{ht})} + m_s^{(\text{bypass}\to\text{ct})}, \quad \forall s \in S, \text{BINT} = 1 \tag{43}$$

Multi-choice mixers on the target side. The cooling and/or heating of stream s exiting the pressure change or bypass stage is enabled within multi-choice mixers for the streams acting as hot (mixer HTM_s) and cold (mixer CTM_s). The mass and heat balance equations of mixer HTM_s are given by Equations (44) and (45).

$$m_s^{(\text{ht})} = \underset{\text{CINT}=1}{m_s^{(\text{comp}\to\text{ht})}} + \underset{\text{EINT}=1}{m_s^{(\text{exp}\to\text{ht})}} + \underset{\text{EINT}=1}{m_s^{(\text{valve}\to\text{ht})}} + \underset{\text{BINT}=1}{m_s^{(\text{bypass}\to\text{ht})}}, \quad \forall s \in S \tag{44}$$

$$m_s^{(\text{ht})} T_s^{(\text{ht,in})} = \underset{\text{CINT}=1}{m_s^{(\text{comp}\to\text{ht})} T_s^{(\text{comp,out})}} + \underset{\text{EINT}=1}{m_s^{(\text{exp}\to\text{ht})} T_s^{(\text{exp,out})}} + \underset{\text{EINT}=1}{m_s^{(\text{valve}\to\text{ht})} T_s^{(\text{valve,out})}} + \underset{\text{BINT}=1}{m_s^{(\text{bypass}\to\text{ht})} T_s^{(\text{bypass})}}, \quad \forall s \in S \tag{45}$$

CTM_s exists within the proposed superstructure for the stream acting as a cold stream, leaving a pressure change or bypass stage mixer. The mass and heat balance equations of mixer CTM_s are given by Equations (46) and (47).

$$m_s^{(\text{ct})} = \underset{\text{CINT}=1}{m_s^{(\text{comp}\to\text{ct})}} + \underset{\text{EINT}=1}{m_s^{(\text{exp}\to\text{ct})}} + \underset{\text{EINT}=1}{m_s^{(\text{valve}\to\text{ct})}} + \underset{\text{BINT}=1}{m_s^{(\text{bypass}\to\text{ct})}}, \quad \forall s \in S \tag{46}$$

$$m_s^{(\text{ct})} T_s^{(\text{ct,in})} = \underset{\text{CINT}=1}{m_s^{(\text{comp}\to\text{ct})} T_s^{(\text{comp,out})}} + \underset{\text{EINT}=1}{m_s^{(\text{exp}\to\text{ct})} T_s^{(\text{exp,out})}} + \underset{\text{EINT}=1}{m_s^{(\text{valve}\to\text{ct})} T_s^{(\text{valve,out})}} + \underset{\text{BINT}=1}{m_s^{(\text{bypass}\to\text{ct})} T_s^{(\text{bypass})}}, \quad \forall s \in S \tag{47}$$

Target mixers (TM_s). In the final TM_s mixer, the hot and cold streams are mixed isothermally as the temperature of the hot and cold streams leaving the heat exchanger is set to the stream target temperature $T_s^{(\text{out})}$. Equation (48) gives the mass balance of mixer TM_s.

$$m_s = m_s^{(\text{ht})} + m_s^{(\text{ct})}, \quad \forall s \in S \tag{48}$$

3.4.2. The HI Model

The HI model M_2 is the simultaneous optimization and heat integration model from Duran and Grossmann [19] based on the pinch location method, where the inequalities given by Equations (49) and (50) constrain the hot utility consumption.

$$q_{\mathrm{HU}} \geq \sum_j f_j \left[\max\left(0, T_j^{(\mathrm{out})} - \left(T_{i'}^{(in)} - \mathrm{HRAT}\right)\right) - \max\left(0, T_j^{(\mathrm{in})} - \left(T_{i'}^{(\mathrm{in})} - \mathrm{HRAT}\right)\right)\right] - \sum_i f_i \left[\max\left(0, T_i^{(\mathrm{in})} - T_{i'}^{(\mathrm{in})}\right) - \max\left(0, T_i^{(\mathrm{out})} - T_{i'}^{(\mathrm{in})}\right)\right], \quad \forall i' \tag{49}$$

$$q_{\mathrm{HU}} \geq \sum_j f_j \left[\max\left(0, T_j^{(\mathrm{out})} - T_{j'}^{(\mathrm{in})}\right) - \max\left(0, T_j^{(\mathrm{in})} - T_{i'}^{(\mathrm{in})}\right)\right] - \sum_i f_i \left[\max\left(0, T_i^{(\mathrm{in})} - \left(T_{i'}^{(\mathrm{in})} + \mathrm{HRAT}\right)\right) - \max\left(0, T_i^{(\mathrm{out})} - \left(T_{j'}^{(\mathrm{in})} + \mathrm{HRAT}\right)\right)\right], \quad \forall j' \tag{50}$$

The cold utility consumption is determined by the global heat balance given by Equation (51).

$$q_{\mathrm{HU}} + \sum_i ec_i = q_{\mathrm{CU}} + \sum_j ec_j \tag{51}$$

where the heat content of the hot (ec_i) and cold (ec_j) streams is given by Equations (52) and (53).

$$ec_i = f_i \left(T_i^{(\mathrm{in})} - T_i^{(\mathrm{out})}\right), \quad \forall i \tag{52}$$

$$ec_j = f_j \left(T_j^{(\mathrm{out})} - T_j^{(\mathrm{in})}\right), \quad \forall j \tag{53}$$

A smooth approximation of the max operators [35] was used to handle discontinuous derivatives in Equations (49) and (50).

3.4.3. The HEN Model

The HEN model (M_3) is based on the superstructure shown in Figure 4, which originated from the HEN model in Floudas et al. [33]. The initial hot stream splitter (S_i) enables stream splitting for a parallel configuration of heat exchangers. The mass balance of splitter S_i is given by Equation (54).

$$f_i = \sum_j f_{i,j}^{(\mathrm{in}\to\mathrm{ehs})} + f_i^{(\mathrm{bypass})}, \quad \forall i \tag{54}$$

The mixers (EM_i) and splitters (ES_i) for the heat exchangers enable the connection between the heat exchangers, facilitating different heat exchange configurations (serial and parallel). The mass and heat balances of mixer EM_i are given by Equations (55) and (56). Equation (57) gives the mass balance of splitter ES_i.

$$f_{i,j}^{(\mathrm{ehs})} = f_{i,j}^{(\mathrm{in}\to\mathrm{ehs})} + \sum_{\substack{j' \\ j'\neq j}} f_{j,i,j'}^{(\mathrm{ehs})}, \quad \forall i, \forall j \tag{55}$$

$$f_{i,j}^{(\mathrm{ehs})} T_{i,j}^{(\mathrm{ehs,in})} = f_{i,j}^{(\mathrm{in}\to\mathrm{ehs})} T_i^{(\mathrm{in})} + \sum_{\substack{j' \\ j'\neq j}} f_{j,i,j'}^{(\mathrm{ehs})} T_{i,j'}^{(\mathrm{ehs,out})}, \quad \forall i, \forall j \tag{56}$$

$$f_{i,j}^{(\mathrm{ehs})} = f_{i,j}^{(\mathrm{ehs}\to\mathrm{out})} + \sum_{\substack{j' \\ j'\neq j}} f_{j',i,j}^{(\mathrm{ehs})}, \quad \forall i, \forall j \tag{57}$$

The fractions of the streams leaving heat exchangers $i-j$ are directed to the final mixer M_i, enabling additional cooling in cooler i−C. The mass and heat balances of mixer M_i are given by Equations (58) and (59).

$$f_i = \sum_j f_{i,j}^{(\text{ehs}\to\text{out})} + f_i^{(\text{bypass})}, \quad \forall i \tag{58}$$

$$f_i T_i^{(\text{m,out})} = \sum_j f_{i,j}^{(\text{ehs}\to\text{out})} T_{i,j}^{(\text{ehs,out})} + f_i^{(\text{bypass})} T_i^{(\text{in})}, \quad \forall i \tag{59}$$

Analogous equations apply for the cold stream superstructure shown in Figure 4b. The mass balance of splitter S_j is given by Equation (60).

$$f_j = \sum_i f_{i,j}^{(\text{in}\to\text{ecs})} + f_j^{(\text{bypass})}, \quad \forall j \tag{60}$$

The mass and heat balances of mixer EM_j are given by Equations (61) and (62). Equation (63) gives the mass balance of splitter ES_j.

$$f_{i,j}^{(\text{ecs})} = f_{i,j}^{(\text{in}\to\text{ecs})} + \sum_{\substack{i' \\ i'\neq i}} f_{i,i',j}^{(\text{ecs})}, \quad \forall i, \forall j \tag{61}$$

$$f_{i,j}^{(\text{ecs})} T_{i,j}^{(\text{ecs,in})} = f_{i,j}^{(\text{in}\to\text{ecs})} T_i^{(\text{in})} + \sum_{\substack{i' \\ i'\neq i}} f_{i,i',j}^{(\text{ecs})} T_{i',j}^{(\text{ecs,out})}, \quad \forall i, \forall j \tag{62}$$

$$f_{i,j}^{(\text{ecs})} = f_{i,j}^{(\text{ecs}\to\text{out})} + \sum_{\substack{i' \\ i'\neq i}} f_{i',i,j}^{(\text{ecs})}, \quad \forall i, \forall j \tag{63}$$

The fractions of the streams leaving heat exchangers $i-j$ are directed to the final mixer M_j, enabling additional heating in heater H$-j$. The mass and heat balances of mixer M_j are given by Equations (64) and (65).

$$f_j = \sum_i f_{i,j}^{(\text{ecs}\to\text{out})} + f_j^{(\text{bypass})}, \quad \forall j \tag{64}$$

$$f_j T_j^{(\text{m,out})} = \sum_j f_{i,j}^{(\text{ecs}\to\text{out})} T_{i,j}^{(\text{ecs,out})} + f_j^{(\text{bypass})} T_j^{(\text{in})}, \quad \forall j \tag{65}$$

For the individual heat exchangers $i-j$, Equations (66) and (67) define the heat balance equations for the hot and cold streams.

$$q_{i,j} = f_{i,j}^{(\text{ehs})} \left(T_{i,j}^{(\text{ehs,in})} - T_{i,j}^{(\text{ehs,out})} \right), \quad \forall i, \forall j \tag{66}$$

$$q_{i,j} = f_{i,j}^{(\text{ecs})} \left(T_{i,j}^{(\text{ecs,out})} - T_{i,j}^{(\text{ecs,in})} \right), \quad \forall i, \forall j \tag{67}$$

The heat balance for cooler $i-\text{C}$ is given by Equation (68), and Equation (69) gives the heat balance for heater H$-j$.

$$q_i^{(\text{C})} = f_i \left(T_i^{(\text{m,out})} - T_i^{(\text{out})} \right), \quad \forall i \tag{68}$$

$$q_j^{(\text{H})} = f_j \left(T_j^{(\text{out})} - T_j^{(\text{m,out})} \right), \quad \forall i \tag{69}$$

The global heat balances for hot stream i and cold stream j are given by Equations (70) and (71).

$$f_i \left(T_i^{(\text{in})} - T_i^{(\text{out})} \right) = \sum_j q_{i,j} + q_i^{(\text{C})}, \quad \forall i \tag{70}$$

$$f_j \left(T_j^{(\text{out})} - T_j^{(\text{in})} \right) = \sum_i q_{i,j} + q_j^{(\text{H})}, \quad \forall j \tag{71}$$

The temperature constraints for the exchangers are given by constraints (72)–(77).

$$\Delta Th_{i,j} \leq T_{i,j}^{(\text{ehs,in})} - T_{i,j}^{(\text{ecs,out})} + \Gamma(1 - z_{i,j}), \quad \forall i, \forall j \tag{72}$$

$$\Delta Tc_{i,j} \leq T_{i,j}^{(\text{ehs,out})} - T_{i,j}^{(\text{ecs,in})} + \Gamma(1 - z_{i,j}), \quad \forall i, \forall j \tag{73}$$

$$\Delta Th_{i}^{(\text{C})} \leq T_{i}^{(\text{m,out})} - T_{\text{CU}}^{(\text{out})} + \Gamma(1 - z_{i}), \quad \forall i \tag{74}$$

$$\Delta Tc_{i}^{(\text{C})} \leq T_{i}^{(\text{out})} - T_{\text{CU}}^{(\text{in})} + \Gamma(1 - z_{i}), \quad \forall i \tag{75}$$

$$\Delta Th_{j}^{(\text{H})} \leq T_{\text{HU}}^{(\text{in})} - T_{j}^{(\text{out})} + \Gamma(1 - z_{j}), \quad \forall j \tag{76}$$

$$\Delta Tc_{j}^{(\text{H})} \leq T_{\text{HU}}^{(\text{out})} - T_{j}^{(\text{m,out})} + \Gamma(1 - z_{j}), \quad \forall j \tag{77}$$

Constraints (78)–(82) apply to the existence of equipment in the optimal design, and constraints (83) and (84) are related to the existence of hot and cold stream branches connected to the heat exchangers.

$$q_{i,j} \leq q_{i,j}^{(\text{ub})} z_{i,j}, \quad \forall i, \forall j \tag{78}$$

$$q_{i}^{(\text{C})} \leq q_{i}^{(\text{C,ub})} z_{i}, \quad \forall i \tag{79}$$

$$q_{j}^{(\text{H})} \leq q_{j}^{(\text{H,ub})} z_{j}, \quad \forall j \tag{80}$$

$$W_{s,k}^{(\text{comp})} \leq W_{s,k}^{(\text{comp,ub})} z_{s,k}^{(\text{comp})}, \quad \forall s, \forall k \tag{81}$$

$$W_{s,k}^{(\text{exp})} \leq W_{s,k}^{(\text{exp,ub})} z_{s,k}^{(\text{exp})}, \quad \forall s, \forall k \tag{82}$$

$$f_{i,j}^{(\text{ehs})} \leq f_{i,j}^{(\text{ehs,ub})} z_{i,j}, \quad \forall i, \forall j \tag{83}$$

$$f_{i,j}^{(\text{ecs})} \leq f_{i,j}^{(\text{ecs,ub})} z_{i,j}, \quad \forall i, \forall j \tag{84}$$

In addition, inequality constraints (85)–(88) are related to the inlet and outlet temperatures of the hot and cold streams in the heat exchangers, coolers and heaters, respectively.

$$T_{i,j}^{(\text{ehs,in})} \geq T_{i,j}^{(\text{ehs,out})}, \quad \forall i, \forall j \tag{85}$$

$$T_{i,j}^{(\text{ecs,in})} \leq T_{i,j}^{(\text{ecs,out})}, \quad \forall i, \forall j \tag{86}$$

$$T_{i}^{(\text{m,out})} \geq T_{i}^{(\text{out})}, \quad \forall i \tag{87}$$

$$T_{j}^{(\text{m,out})} \leq T_{j}^{(\text{out})}, \quad \forall j \tag{88}$$

3.5. Objective Function

The objective function is given by Equation (89) for the combined NLP model ($M_1 + M_2$), which includes the operational cost for energy (electricity and hot and cold utilities).

$$\min Z_1 = \sum_{\substack{s,k \\ \text{CINT} = 1}} W_{s,k}^{(\text{comp})} C_{\text{el}}^{(\text{cons})} - \sum_{\substack{s,k \\ \text{EINT} = 1}} W_{s,k}^{(\text{exp})} C_{\text{el}}^{(\text{prod})} + q_{\text{HU}} C_{\text{HU}} + q_{\text{CU}} C_{\text{CU}} \tag{89}$$

The objective function of the MINLP model ($M_1 + M_3$) for a simultaneous WHEN is given by Equation (90), which includes the operational cost for energy (electricity and hot and cold utilities) and the investment cost for the equipment (compressors, turbines and heat exchangers). The investment cost for the valves is considered negligible in this study.

$$\min Z_2 = \sum_{\substack{s,k \\ \text{CINT}=1}} W_{s,k}^{(\text{comp})} C_{\text{el}}^{(\text{cons})} - \sum_{\substack{s,k \\ \text{EINT}=1}} W_{s,k}^{(\text{exp})} C_{\text{el}}^{(\text{prod})} + \sum_i q_i^{(\text{C})} C_{\text{CU}} + \sum_j q_j^{(\text{H})} C_{\text{HU}}$$
$$+ af \left(\text{FBM}_{\text{comp}} \sum_{\substack{s,k \\ \text{CINT}=1}} \left(az_{\text{comp}} + b \left(W_{s,k}^{(\text{comp})} \right)^n \right) + \text{FBM}_{\text{exp}} \sum_{\substack{s,k \\ \text{EINT}=1}} \left(az_{\text{exp}} + b \left(W_{s,k}^{(\text{exp})} \right)^n \right) \right. \quad (90)$$
$$\left. + \text{FBM}_{\text{exc}} \sum_{i,j} \left(az_{i,j} + bA_{i,j}^n \right) + \text{FBM}_{\text{exc}} \sum_i (az_i + bA_i^n) + \text{FBM}_{\text{exc}} \sum_j \left(az_j + bA_j^n \right) \right)$$

where the heat transfer areas for the heat exchangers, coolers and heaters are given as follows, using Chen's approximation of the logarithmic mean temperature difference [36,37]:

$$A_{i,j} = \frac{q_{i,j} \left(\frac{1}{h_i} + \frac{1}{h_j} \right)}{\left(\Delta Th_{i,j} \Delta Tc_{i,j} \frac{\Delta Th_{i,j} + \Delta Tc_{i,j}}{2} \right)^{1/3}}$$

$$A_i = \frac{q_i^{(\text{C})} \left(\frac{1}{h_i} + \frac{1}{h_{\text{CU}}} \right)}{\left(\Delta Th_i^{(\text{C})} \Delta Tc_i^{(\text{C})} \frac{\Delta Th_i^{(\text{C})} + \Delta Tc_i^{(\text{C})}}{2} \right)^{1/3}}$$

$$A_j = \frac{q_j^{(H)} \left(\frac{1}{h_j} + \frac{1}{h_{\text{HU}}} \right)}{\left(\Delta Th_j^{(\text{H})} \Delta Tc_j^{(\text{H})} \frac{\Delta Th_j^{(\text{H})} + \Delta Tc_j^{(\text{H})}}{2} \right)^{1/3}}$$

The investment annualization factor [38], for a given fractional interest rate (ir) and equipment depreciation period (dp), is obtained from

$$af = \frac{ir(1+ir)^{dp}}{(1+ir)^{dp} - 1}$$

3.6. Model Limitations and Possible Improvements

The following limitations in the proposed model should be addressed in the future development of the model.

- The model only includes pressure manipulation equipment for gaseous streams; to include liquid streams, additional pressure change branches should be included to enable the pumping of fluids and liquid expansion.
- Only one hot and one cold utility is considered, suggesting that the model's extension should integrate the WHEN network with the utility network, enabling the extraction of utilities at different temperature levels.
- Only utility expanders and compressors are considered; there is a need to include SSTCs to enable additional work integration opportunities.
- Realistic efficiencies of compressors and expanders should be considered.
- The phase change (evaporation/condensation) should be considered.

3.7. Solution Approach

The synthesis of WHENs is a non-convex optimization problem that is very difficult to solve as the scale of the problem increases. In this work, two relatively complex su-

perstructures, a WHI superstructure and a HEN superstructure, are entangled. Models related to these superstructures are nonconvex and nonlinear, with a nonlinear objective function including capital investment for the equipment. Thus, finding global or even good local solutions can be quite challenging. To solve the optimization problem, a two-step solution strategy is employed, shown in Figure 5. In the first step, the combined NLP model ($M_1 + M_2$) is solved with the objective function given by Equation (89). The solution from the first step provides efficient initialization for the second MINLP model. In addition, the NLP model identifies hot and cold streams, reducing the number of heat exchanger matches (see Appendix A.2) in the second optimization step. In the second step of the proposed solution strategy, a combined MINLP model ($M_1 + M_3$) is solved with the objective function given by Equation (90). Models $M_1 + M_2$ and $M_1 + M_3$ are connected using equations to identify streams within the WHI superstructure presented in Appendix A.1. The model is developed in the GAMS [39] and solved with Conopt4/Ipopt/Snopt as the NLP solvers for the first NLP model and SBB as the MINLP solver with Conopt4 as a subsolver. The model can be solved in iterations (optional) or multiple runs by assigning new values for HRAT in each run, providing different initial solutions for the MINLP model and generating a set of local solutions from which the best one can be selected.

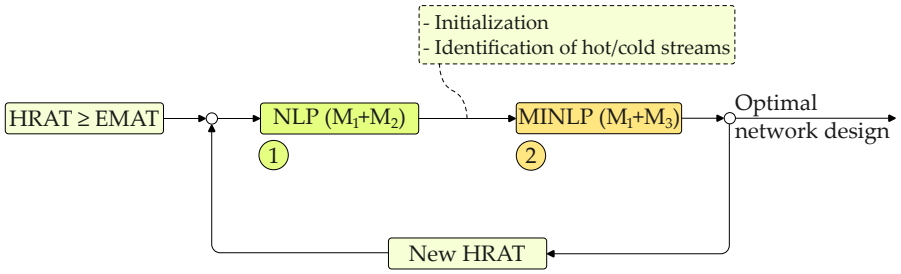

Figure 5. Strategy for solving the optimization problem.

4. Examples

This section provides four examples to demonstrate the methodology and analyze the impacts of the electricity cost, equipment cost and annualized investment cost on the optimal network design. Table 1 gives the parameters and utility cost data for the studied examples, and Table 2 shows the equipment cost data. The cost data from the literature are normalized to the same year (2022) using the Chemical Engineering Plant Cost Index (CEPCI), and the data are fitted to the same model equation $a + bS^n$, where a, b and n are coefficients, and S is the equipment attribute. The nonlinear regression software Sigma Plot v 14.0 [40] is used for data fitting.

Table 1. Parameters and cost data for the studied examples.

Parameter	Unit	Examples 1–3	Example 4
Heating utility cost	k$/kWy	0.377	0.337
Cooling utility cost	k$/kWy	0.1	0.1
Electricity cost (consumed)	k$/KWy	0.45505	0.45505
Electricity cost (produced)	k$/KWy	0.45505	0.36403
Joule–Thompson coefficient of expansion	K/MPa	1.961	-
Isentropic efficiency	-	1	1

Table 2. Equipment cost data in k$ adjusted with CEPCI = 819 for 2022.

Reference	*S* Range	Equipment	*a*	*b*	*n*	R^2
Seider et al. [41]	149–22,371	COMP	-	4.0422	0.8	1
	15–3728	EXP	-	1.1097	0.81	1
	4–1115	STHE	23.0784	0.1165	1	0.9989
			20.7139	0.208	0.9166	1
Peters et al. [42]	75–3000	COMP	-	1.8337	0.9435	1
	100–3000	EXP	-	6.9313	0.5889	1
	10–1000	STHE	12.342	0.17	1	0.9991
			9.0307	0.2889	0.9239	0.9997
Couper et al. [43]	149–22,371	COMP	-	19.235	0.62	1
	15–3728	EXP	-	0.9731	0.81	1
	14–1115	STHE	7.0232	0.2479	1	0.9996
			9.5624	0.1785	1.0469	0.9999
Woods [44]	2–4000	COMP	-	2.198	0.9	1
	746–22,371	EXP	-	1.7929	0.8	1
	20–1150	STHE	-	2.8628	0.65	1
Towler and Sinnott [45]	75–30,000	COMP	888.122	30.625	0.6	1
	1000–15,000	EXP *	1026.8	0.1968	1	1
	10–1000	STHE	49	0.1072	1.2	1
Turton [46]	450–3000	COMP	-	4.2380	0.71	0.9993
	100–3000	EXP	−2140.823	1641.81	0.0712	0.9983
	20–1000	STHE	34.1951	0.0876	1.1532	0.9999

* Shah et al. [47]. For compressors and expanders, the equipment attribute is in kW; for heat exchangers, it is in m^2

4.1. Example 1

This example considers the integration of compressors into a HEN, optimizing the compressor inlet temperature. Data for this example are taken from the literature [4] and presented in Table 3. Only the S2 stream is pressure-changing, while S1 and S3 are non-pressure-changing streams. All streams are considered an ideal gas with polytropic exponent $k = 1.4$. The EMAT is set to be 20 K. In addition, the annualization factor for the investment is calculated for an interest rate of 8% over a period of 10 years. The example is solved by considering the different investment cost equations given in Table 2. In addition, a basic sensitivity analysis is performed, comparing the network designs for different electricity costs.

Table 3. Stream data for Example 1.

Stream	$T_s^{(in)}$ (K)	$T_s^{(out)}$ (K)	mc_p (kW/K)	$p_s^{(in)}$ (MPa)	$p_s^{(out)}$ (MPa)	h (kW/m^{2}K)
S1	637	333	2	0.1	0.1	0.1
S2	288	523	1	0.1	0.3	0.1
S3	472	543	4	0.1	0.1	0.1
HU	673	673	-	-	-	1
CU	288	288	-	-	-	1

Table 4 shows the optimization results for Example 1 using different equipment cost equations from Table 2. Note that the key performance indicators (utility consumption and OPEX) are the same in all cases, resulting in the same network design. However, the CAPEX is shown to be significantly different for the four cases; thus, the TAC can be overestimated or underestimated, showing the importance of having quality cost data.

Table 4. Network performance indicators for Example 1 with different cost equations.

Indicator	Unit	Seider et al. [41]	Couper et al. [43]	Peters et al. [42]	Towler and Sinnott [45]
No. of HEs	-	5	5	5	5
No. of COMP	-	1	1	1	1
HU demand	kW	235.587	235.587	235.587	235.587
CU demand	kW	135	135	135	135
Compression work	kW	174.41	174.41	174.41	174.41
Total CAPEX	k$	407.928	598.092	363.073	1908.525
CAPEX	k$/y	60.685	89.133	54.109	284.427
OPEX	k$/y	181.683	181.683	181.683	181.683
TAC	k$/y	242.368	270.816	235.792	466.110

References point to the cost equations in Table 2.

Figure 6 shows the optimal network design for Example 1. The S1 stream is a hot stream cooled at a constant pressure in two heat exchangers (with heat loads 360 kW and 185 kW) and one cooler (135 kW) to obtain the stream target temperature. The S2 stream is not compressed at the lowest temperature but at the pinch temperature. Thus, the S2 stream changes its identity; stream S2 is cold before and hot after the compression. The compression heat is used to preheat the cold S3 stream. The S3 stream is a cold stream integrated within two parallel heat exchangers (with heating loads of 360 kW and 124.41 kW); additionally, a heater is required with a heat load of 235.59 kW to meet the stream's target temperature.

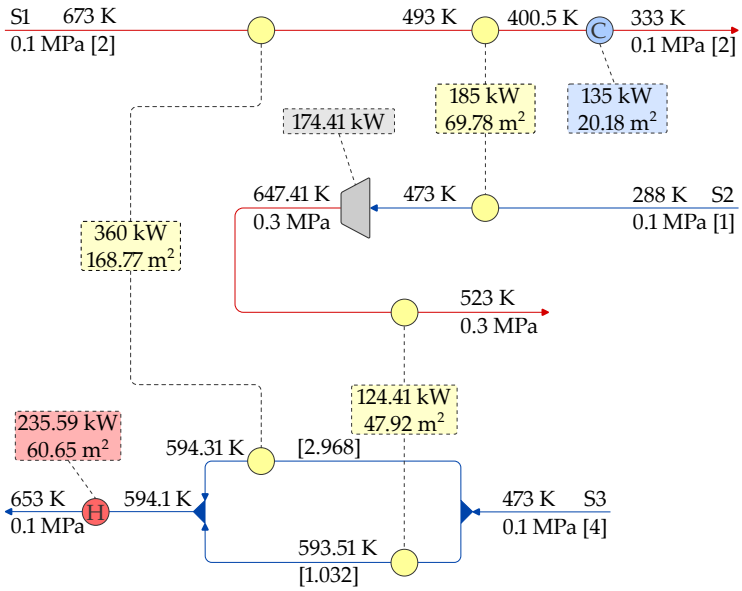

Figure 6. Optimal network design for Example 1.

Table 5 compares the results of two case studies presented in the literature by Fu and Gundersen [4] with our approach. Case A is a network design where compression starts at ambient temperature, and Case B is compression at the pinch, as suggested by the proposed pinch methodology in their work, minimizing the exergy consumption of the system. The network design in this work is the same as in Case B, with very small, negligible differences in the network design parameters, possibly related to rounding errors.

Table 5. Network performance indicators for Example 1.

Indicator	Unit	Fu and Gundersen [4] Case A	Fu and Gundersen [4] Case B	This Work
HU demand	kW	410	235.5	235.59
CU demand	kW	241.3	135.0	135.0
Compression work	kW	106.3	174.5	174.41
Exergy consumption	kW	340.8	309.2	309.2
Total CAPEX	k$	1742.0	1908.73	1908.52
CAPEX	k$/y	259.610	284.457	284.427
OPEX	k$/y	227.073	181.691	181.683
TAC	k$/y	486.682	466.148	466.110

In addition, a basic sensitivity analysis is performed for a value that is ±50% of the base value for electricity cost (0.45505 k$/kWy). The optimization results are presented in Table 6. For an electricity cost that is −50% of the base value, the optimal network design is the same as for the base electricity cost. However, for an electricity cost of +50% of the base electricity cost, the optimal network design (Figure 7a) exhibits reduced work consumption (106.2 kW compared to 174.41 kW for the base cost design) due to the compression of stream S2 at ambient temperature. This reduces the heat recovery as the stream leaving the compressor now acts as a cold stream requiring heating; thus, increased utility consumption is needed. Compared to the solution obtained by Fu and Gundersen [4] for the case of ambient compression (see Figure 7b), the optimum network design exhibits the same exergy consumption (340.8 kW) but a slightly lower TAC (501.723 k$/y compared to 506.375 k$/y) due to the reduced number of heat exchangers and thus the HEN investment cost.

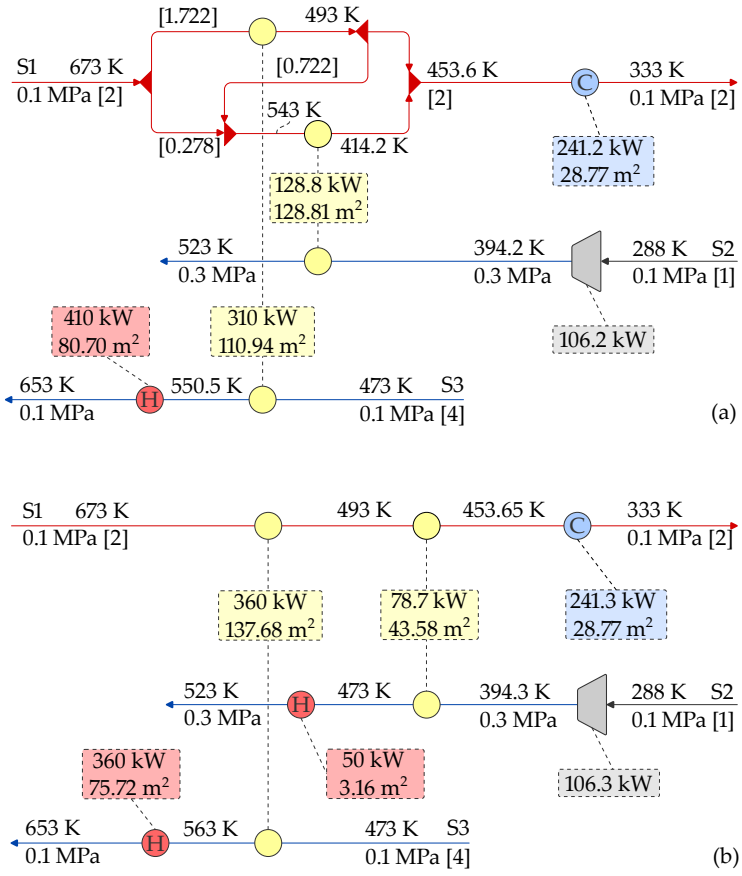

Figure 7. Optimal network design for Example 1 considering electricity cost of 0.6826 $/kWy. (**a**) Optimum design in this paper, (**b**) optimum design from Fu and Gundersen [4] Case A.

Table 6. Sensitivity analysis for Example 1 regarding electricity cost.

Indicator	Unit	Electricity Cost (k$/kWy)		
		0.2275	**0.45505**	**0.6826**
No. of HEs	-	5	5	4
HU demand	kW	235.59	235.59	410
CU demand	kW	135.0	135.0	241.2
Compression work	kW	174.41	174.41	106.2
Exergy consumption	kW	309.2	309.2	340.74
Total CAPEX	k$	1908.52	1908.52	1681.17
CAPEX	k$/y	284.427	284.427	250.543
OPEX	k$/y	141.995	181.683	251.18
TAC	k$/y	426.422	466.110	501.723

4.2. Example 2

This example considers the integration of expanders into the HEN, optimizing the expander inlet temperature. Data for this example are taken from the literature [5] and presented in Table 7. Only the S1 stream is pressure-changing, while S2, S3 and S4 are non-pressure-changing hot and cold streams. All streams are considered ideal gases with polytropic exponent $k = 1.4$. The EMAT is set to be 20 K. In addition, the investment annualization factor is varied from 0.08 to 1 to analyze its impact on the optimal network design. Equipment cost data are based on the equation from Couper et al. [43] presented in Table 2.

Table 7. Stream data for Example 2.

Stream	$T_s^{(in)}$ (K)	$T_s^{(out)}$ (K)	mc_p (kW/K)	$p_s^{(in)}$ (MPa)	$p_s^{(out)}$ (MPa)	h (kW/m^{2}K)
S1	673	333	3	0.3	0.1	0.1
S2	603	353	9	0.1	0.1	0.1
S3	288	493	6	0.1	0.1	0.1
S4	413	653	8	0.1	0.1	0.1
HU	673	673	-	-	-	1
CU	288	288	-	-	-	1

Table 8 shows the optimization results for the optimal designs with different annualization factor values. Lower values of the annualization factor (e.g., 0.08) give designs with higher total investment costs for the expanders and compressors. However, the annualized investment cost is lower because the investment is distributed over a longer depreciation time. In addition, the hot and cold utility consumption is minimal compared to other solutions. The annualization factor is a trade-off parameter between the operational and investment costs; increasing the annualization factor places more weight on the investment, and, thus, the total investment decreases while the annualized investment increases. This reduces the work produced in the expander and increases the hot and cold utility consumption. Thus, for a value of $af = 1$, we have the lowest total investment cost, corresponding to the minimum work produced and the highest utility consumption. However, because the total investment is the lowest, we have a simpler network design with fewer heat exchangers.

Table 8. Optimal network performance indicators for Example 2. A comparison regarding different annualization factors.

Indicator	Unit	Annualization Factor					
		0.08	**0.1**	**0.2**	**0.3**	**0.5**	**1**
No. of HE		9	9	7	7	6	6
HU demand	kW	350	350	350	366.55	401.46	491.70
CU demand	kW	67.07	67.14	81.44	98.99	153.09	243.33
Expansion work	kW	402.93	402.86	388.56	387.55	368.37	368.37
Total CAPEX	k$	644.88	643.857	598.897	567.351	493.432	435.125
CAPEX	k$/y	51.59	64.386	119.779	170.205	246.716	435.125
OPEX	k$/y	−44.696	−44.658	−36.721	−28.268	−0.965	42.079
TAC	k$/y	6.894	19.727	83.058	141.937	245.751	477.204

Figure 8 shows the optimal network design with the annualization factor $af = 0.1$. The S1 stream is a hot stream cooled to almost 498 K in a series of two heat exchangers with heat loads of 210 kW and 313.59 kW, respectively, and then expanded from 0.3 MPa to 0.1 MPa, producing 402.86 kW of work. An additional heat exchanger with a load of 26.41 kW and a cooler with a load of 67.14 kW are placed after the expander to reach the target temperature of 333 K. The S2 stream is cooled in a series of four heat exchangers (with a total heat load of 2250 kW). The S3 stream is completely integrated within a series of four heat exchangers (with a total heat load of 1230 kW), without external heating or cooling, while the S4 cold stream requires a series of three heat exchangers (with a total heat load of 1570 kW) and an additional heater with a heat load of 350 kW. The optimal network design consists of a total of seven heat exchangers (heat recovery 2800 kW), one heater (350 kW) and one cooler (67.14 kW). Figure 9 shows the optimal network design for a case with an annualization factor of 0.2. The optimal network design now has fewer heat exchangers (7 vs. 9), less work produced and more utilities consumed, for the reasons previously explained. Figure 10 shows an even simpler optimal network design for an annualization factor $af = 1$, with the additional expense in the OPEX and significantly increased utility consumption, where the income from expansion no longer covers the hot and cold utility costs, as indicated by the positive OPEX value in the last column of Table 8.

Table 9 compares the results with those from the literature [5]. The previous authors presented an exergy-pinch-based methodology to find the optimum network design with the minimum exergy consumed by the system. Different cases, A, B and C, correspond to different network designs based on the proposed set of rules for the expansion of streams at different temperatures. The cost for the network designs has been recalculated based on their optimal design. Network design C (Example 5, Case C in their work [5]) has the lowest exergy consumption (but the highest exergy production) but, interestingly, also the lowest TAC of the three designs. However, because the authors did not minimize the TAC of the network, our design exhibits a lower TAC, with fewer heat exchangers and only one expander, but with increased exergy consumption (decreased exergy production).

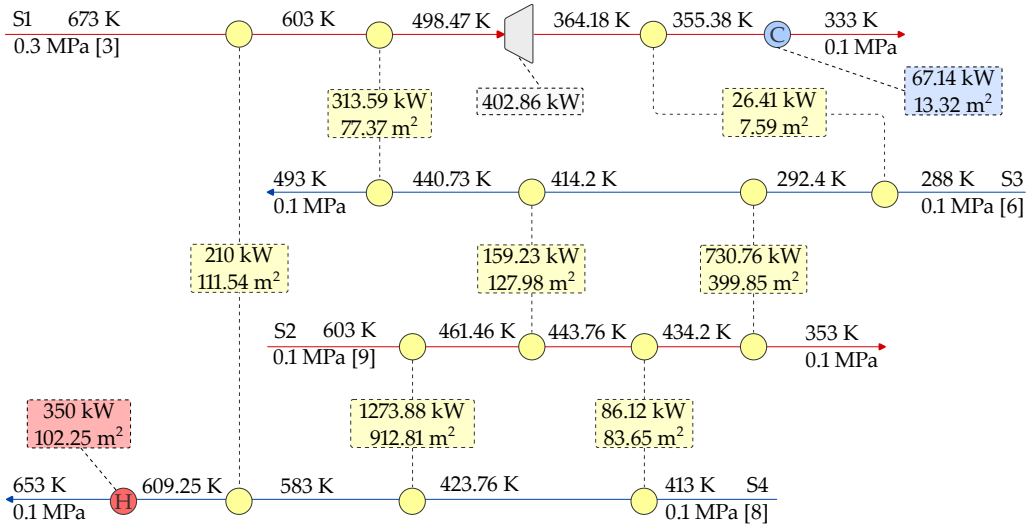

Figure 8. Optimal network design for Example 2 ($af = 0.1$).

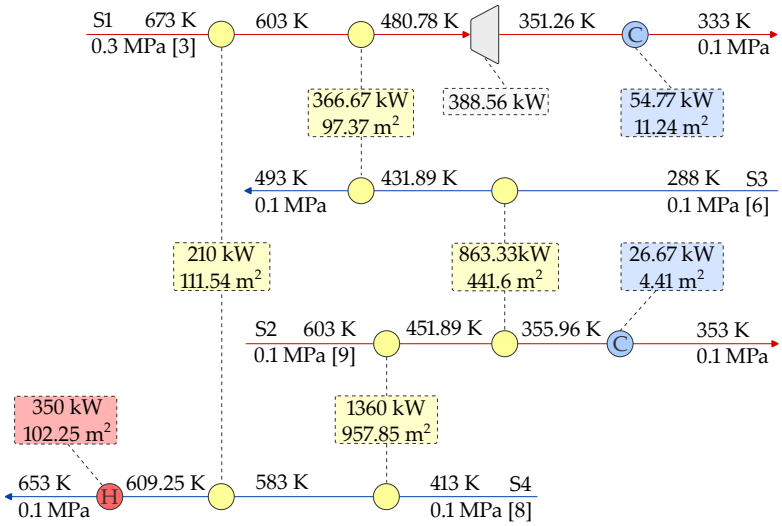

Figure 9. Optimal network design for Example 2 ($af = 0.2$).

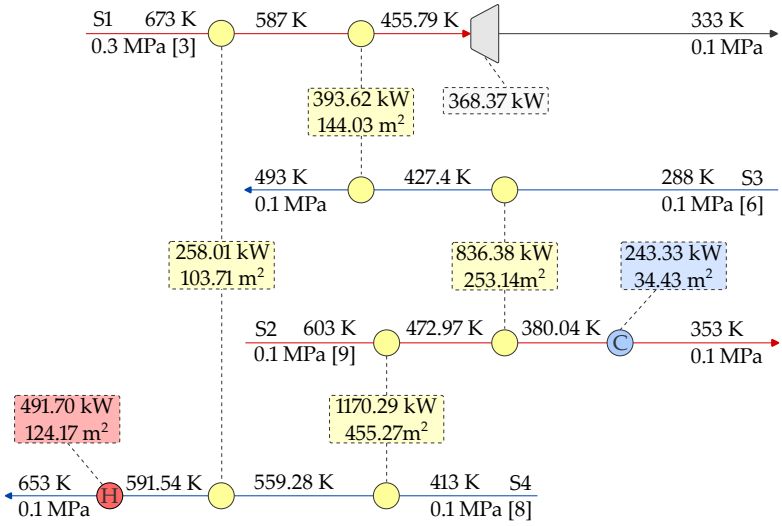

Figure 10. Optimal network design for Example 2 ($af = 1$).

Table 9. Network performance indicators and results comparison for Example 2 ($af = 0.1$).

Indicator	Unit	Fu and Gundersen [5] Case A	Fu and Gundersen [5] Case B	Fu and Gundersen [5] Case C	This Work
No. of HEs	-	7	8	9	7
No. of EXP	-	1	1	2	1
HU demand	kW	694	637.5	350	350
CU demand	kW	270	270	63.5	67.14
Expansion work	kW	543.9	487.5	406.6	402.86
Exergy consumption	kW	−147.0	−122.9	−206.4	−188.34
Total CAPEX	k$	651.771	599.452	772.952	643.857
CAPEX	k$/y	65.177	59.945	77.295	64.386
OPEX	k$/y	41.131	45.496	−46.727	−44.658
TAC	k$/y	106.308	105.441	30.568	19.727

4.3. Example 3

In this example, compression and expansion are considered simultaneously. The stream data for Example 3 are given in Table 10, provided from the literature [48], with the equipment cost data given in Table 2, using the cost equations from Couper et al. [43] and Towler and Sinnott [45]. In addition, we consider the direct and indirect installed costs for the equipment accounted for by bare module factors $FBM_{exc} = 3.29$, $FBM_{comp} = 2.8$ and $FBM_{exp} = 3.5$ from the literature [46]. The annualization factor for the investment is 0.18. The isentropic efficiency of the compressors and expanders is 1, and The EMAT is 20 K.

Table 10. Stream data for Example 3.

Stream	$T_s^{(in)}$ (K)	$T_s^{(out)}$ (K)	mc_p (kW/K)	$p_s^{(in)}$ (MPa)	$p_s^{(out)}$ (MPa)	h (kW/m^{2}K)
S1	673	308	2	0.2	0.1	0.1
S2	593	433	4	0.1	0.1	0.1
S3	383	308	3	0.1	0.1	0.1
S4	288	653	3	0.1	0.2	0.1
S5	463	523	10	0.1	0.1	0.1
HU	673	673	-	-	-	1
CU	288	288	-	-	-	1

Figure 11 shows the optimal network design with the minimum TAC for the cost equation from Couper et al. [43]. The optimal design exhibits a rather complicated network including five heat exchangers, one heater and two coolers, with hot and cold utility consumption of 350.61 kW and 304.92 kW, respectively. The expansion of stream S1 starts at 375.46 K (the work produced is 134.91 kW) with the outlet stream at the required target temperature. The compression of stream S4 starts at ambient temperature, 288 K, with the work consumed being 189.23 kW. Interestingly, stream S3 is not integrated because it is the hot stream at the lowest temperature and requires cooling of 225 kW. The OPEX of the network is 187.387 k$/y with an annualized investment of 409.508 k$/y. The TAC of the network is 596.895 k$/y.

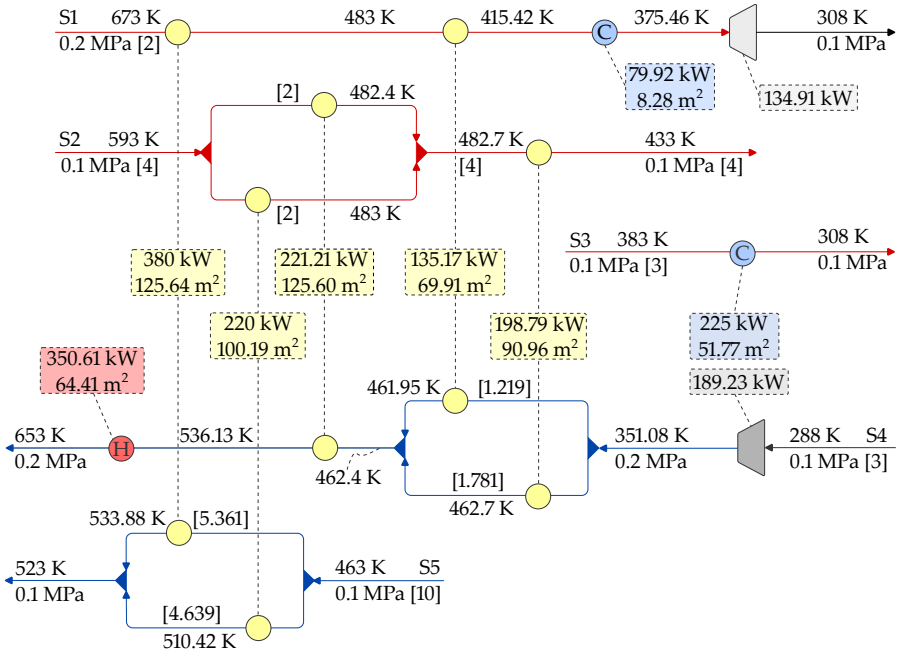

Figure 11. Optimal network design for Example 3 (cost equation from Couper et al. [43] with $af = 0.18$).

Example 3 is also solved using a different cost equation from Towler and Sinnott [45] in Table 2, showing that the selection of the cost equation does affect the optimal design, in contrast to the solutions obtained for Example 1, where all cost equations considered gave the same optimal network design. Figure 12 shows the optimal network design in this case. This design is much simpler, including three heat exchangers, one heater and two coolers, with hot and cold utility consumption of 485.77 kW and 401.44 kW, respectively. The expansion of stream S1 now starts at a higher temperature of 483 K (the work produced is 173.55 kW vs. 134.9 kW), with the outlet stream requiring additional cooling (176.44 kW) to achieve the target temperature. The compression of stream S4 also starts at ambient temperature, 288 K, for a total amount of work consumed of 189.23 kW (the same as in the design shown in Figure 11). Stream S3 is not integrated. Table 11 compares the results with the literature, where the authors [48] presented three cases of optimal designs using a systematic approach based on thermodynamic insights to minimize the exergy consumption of the system. The cost for their designs was recalculated using the cost data provided for this example.

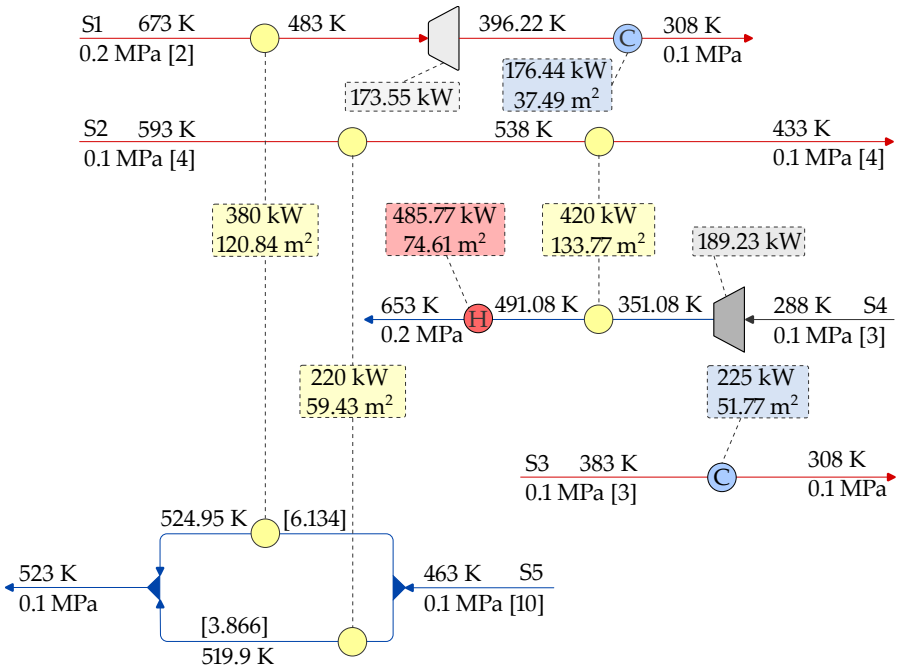

Figure 12. Optimal network design for Example 3 (cost equation from Towler and Sinnott [45] with $af = 0.18$).

Table 11. Network performance indicators for Example 3 (cost equation from Towler and Sinnott [45]).

Indicator	Unit	Fu and Gundersen [48] Case I	Fu and Gundersen [48] Case II	Fu and Gundersen [48] Case III	This Work
No. of HEs	-	8	8	11	6
No. of EXP	-	1	1	2	1
No. of COMP	-	1	1	2	1
Hot utility demand	kW	591.8	119.4	37.6	485.71
Cold utility demand	kW	439.4	150	91.7	225
Compression work	kW	189.3	304.2	312.4	189.23
Expansion work	kW	241.8	173.6	158.3	173.55
Exergy consumption	kW	286.0	198.9	175.6	293.6
Total CAPEX	k$	10,037.51	10,824.71	18,246.25	9574.04
CAPEX	k$/y	1806.75	1948.45	3284.32	1723.33
OPEX	k$/y	243.120	119.445	93.45	230.392
TAC	k$/y	2049.87	2067.89	3377.794	1953.742

In addition, we use the cost equation from Towler and Sinnott [45], with the annualization factor now having a value $af = 0.08$. This places more weight on the operational expenditures, and, as a result, we have an entirely different network design with a reduced OPEX compared to the solution with $af = 0.18$. The optimal network design shown in Figure13 exhibits cold utility consumption of only 96.02 kW, without using hot utilities. This results in a network design requiring much more compression power (351.96 kW vs. 189.23 kW). Expansion starts at a lower temperature; thus, the work produced is reduced (155.94 kW vs. 177.55 kW). Notice that the S3 stream is fully integrated and does not require cold utilities. The TAC of this optimal design is 973.29 k$/y, compared to the best design from Fu and Gundersen [48] (Case II recalculated for $af = 0.08$), with a TAC 985.42 k$/y. The difference in cost is about 1.2%. The reason for the much smaller difference in cost is that the designs from Fu and Gundersen [48] favor the cases in which less weight is placed on the investment cost. In these cases, their methodology gives very good results (cost-wise), even if the objective is to minimize the exergy consumption.

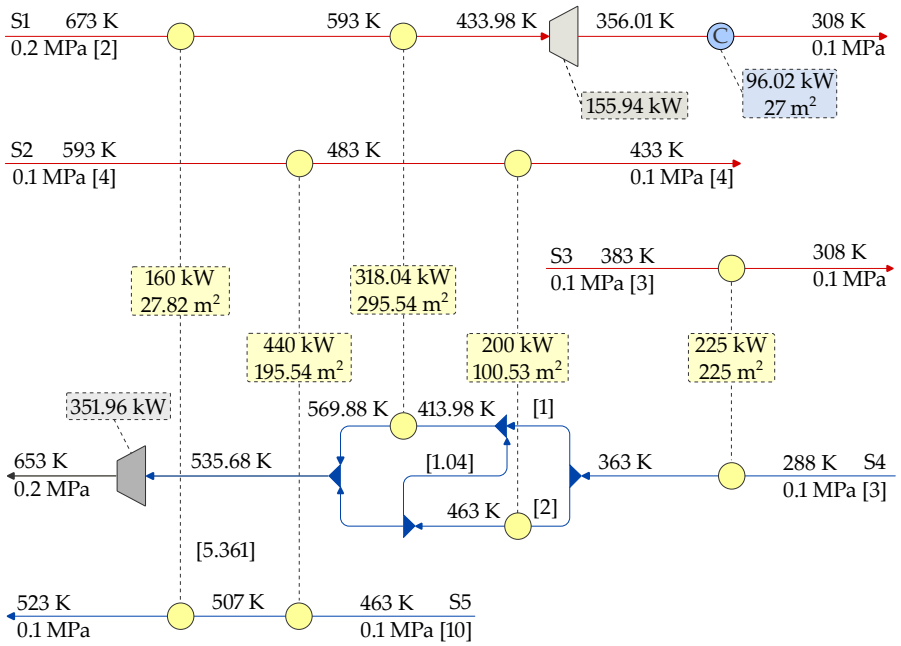

Figure 13. Optimal network design for Example 3 (cost equation from Towler and Sinnott [45] with $af = 0.08$).

4.4. Example 4

The previous example considered both compression and expansion simultaneously. However, only one stream is expanded, and one stream is compressed. Thus, Yu et al. [34] modified Example 3 to create a problem wherein all streams are subject to a pressure change. In addition, the supply and target temperatures are the same for all streams, so it is unclear which streams should be hot or cold before optimization. The proposed superstructure in this work enables the handling of unclassified streams; each can be hot or cold before and after the pressure change stages. The stream data for this example are given in Table 12. In addition, to compare the results, the cost data given in Table 13 are provided from the literature [27]. The original cost equation for the heat exchangers in the reference is $93,500.12 + 602.96A + 0.149A^2$ and is converted to the standardized model $a + bA^n$ used in this paper. The R^2 of the fit is 0.9999, making the error negligible compared to the original equation. The annualization factor for the capital investment is 0.18. The isentropic efficiency of the compressors and expanders is 1. The exchanger's minimum approach temperature is 20 K.

Table 12. Stream data for Example 4.

Stream	$T_s^{(in)}$ (K)	$T_s^{(out)}$ (K)	mc_p (kW/K)	$p_s^{(in)}$ (MPa)	$p_s^{(out)}$ (MPa)	h (kW/m^{2}K)
S1	623	623	2	0.2	0.1	0.1
S2	593	593	4	0.2	0.1	0.1
S3	383	383	3	0.2	0.1	0.1
S4	323	323	3	0.1	0.2	0.1
S5	463	463	10	0.1	0.2	0.1
HU	673	673	-	-	-	1
CU	288	288	-	-	-	1

Table 13. Cost data for equipment and utilities for Example 4.

Reference	Equipment	a	b	n
Lin et al. [27]	COMP	-	51,104.85	0.62
	EXP	-	2585.47	0.81
	STHE	99,163	250.9	1.1577
Cost Parameter	$C_{el}^{(cons)}$	$C_{el}^{(prod)}$	C_{HU}	C_{CU}
\$/kWy	455.05	364.03	337	100

For compressors and expanders, the equipment attribute is in kW; for heat exchangers, it is in m^2. The equipment cost is in \$.

Figure 14 shows the optimal network design obtained using the proposed superstructure and optimization model. The S1 stream's expansion starts at the maximum temperature, producing 223.86 kW of work. The stream leaving the expander is a cold stream requiring heating with hot utilities, with the load equal to the work produced. The S2 stream changes identity, from first being a hot stream cooled before the expansion and then a cold stream after the expansion. The heating of the S2 stream leaving the expander is achieved in two heat exchangers, recovering 209.8 kW of heat in a match with the hot S5 stream and 467.66 kW with the hot S2 stream (self-recuperation). Additional heating (132.34 kW) is required to achieve the stream's target temperature. Stream S3 is expanded at the stream's initial temperature, producing 206.43 kW of work, and the heating of the stream after the expansion is done by heat recovery from the hot stream S5. Because the stream supply and target temperatures are the same, the heat required for heating (206.43 kW) is equal to the work produced by the expander. The S4 stream is not integrated with other streams.

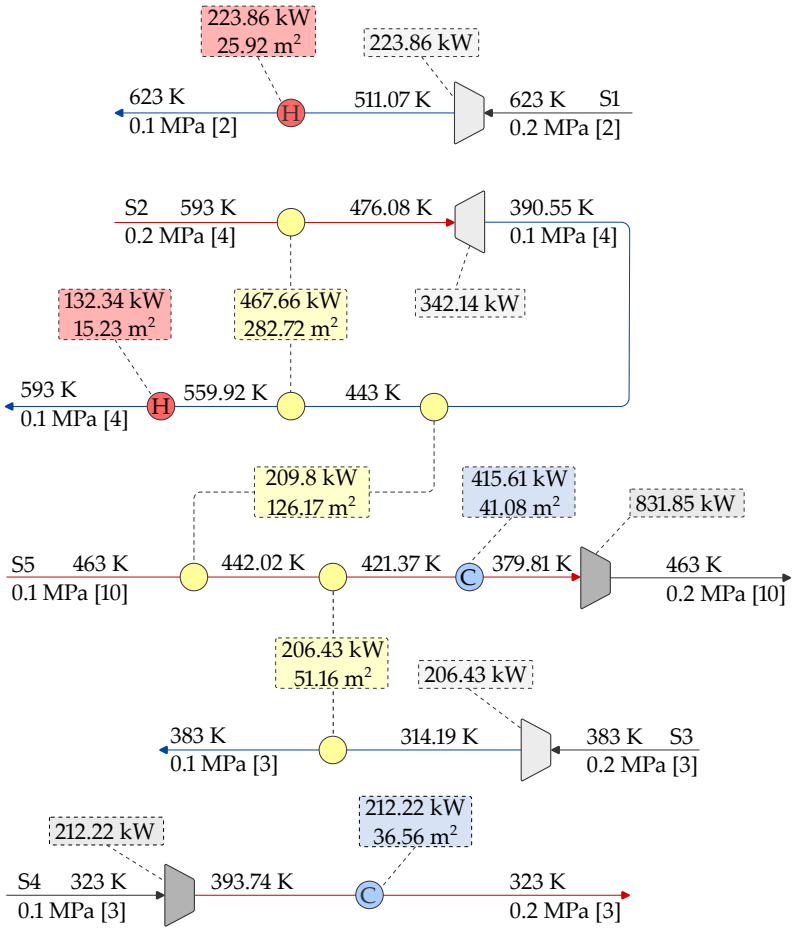

Figure 14. Optimal network design for Example 4.

The compression of the stream is performed at the stream's initial temperature, followed by cooling with cold utilities (212.22 kW). The S5 stream is identified as a hot stream being cooled in a series of two heat exchangers and a cooler to reduce the work consumption in the compressor (831.85 kW). The stream leaves the compressor exactly at the target temperature. Table 14 shows the key network performance indicators and network costs for Example 4. In addition, a comparison of the results with those in the literature is given. Lin et al. [27] presented a global optimization approach for a minimal WHEN network where the heat balance was based on enthalpy calculations using equations of state. The network performance indicators from Lin et al. [27] were thus recalculated using parameters from the optimal design and assuming a constant heat capacity flow rate. The optimal network design obtained by Lin et al. [27] is shown in Figure 15. The TAC for their network using the recalculated values (1549.028 \$/y) given in Table 14 is only slightly different compared to the optimal value in their approach of 1544.845 \$/y. The network design shown in Figure 15 consists of only one heat exchanger, with a heat recovery load of 206.22 kW. This increases the hot and cold utility consumption compared to the design reported in our work. The heat content of S2 is used to produce work and not for heat recovery; thus, more work is produced. Our design exhibits a higher CAPEX due to the higher HEN investment cost, but the OPEX is reduced compared to the work of Lin et al. [27].

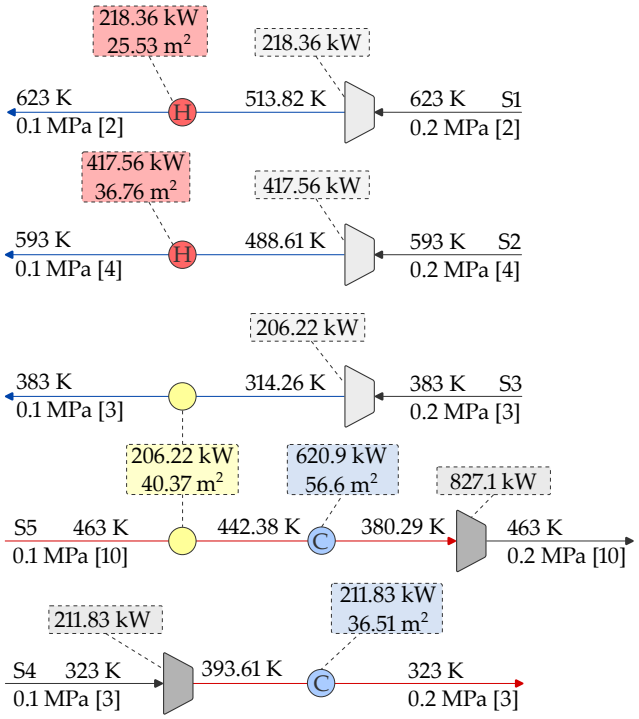

Figure 15. Optimal network design for Example 4 from the literature [27].

Table 14. Network performance indicators for Example 4.

Indicator	Unit	Yu et al. [34]	Lin et al. [27]	This Work
Number of COMP and EXP	-	7	5	5
Number of HE units	-	13	5	10
Hot utility demand	kW	40	635.92	356.2
Cold utility demand	kW	342.7	832.73	627.83
Compression work	kW	1127.3	1038.93	1044.07
Expansion work	kW	827.4	842.14	772.43
Total CAPEX	k\$	9719.198	6029.103	6421.778
CAPEX	k\$/y	1749.455	1085.239	1155.92
OPEX	k\$/y	259.528	463.79	376.749
TAC	k\$/y	2008.983	1549.028	1532.658

However, although the proposed approach used in Lin et al. [27] gives a global solution to their minimal WHEN superstructure, it is still not the global solution to the problem, since their superstructure may not include all possible options for work and heat integration. Using our approach, a set of local solutions can be obtained, as shown in Figure 16, and some of the solutions are practically the same as the solution obtained by Lin et al. [27]. It should also be mentioned that the solution from Yu et al. [34] in Table 14 is based on exergy rather than economy considerations.

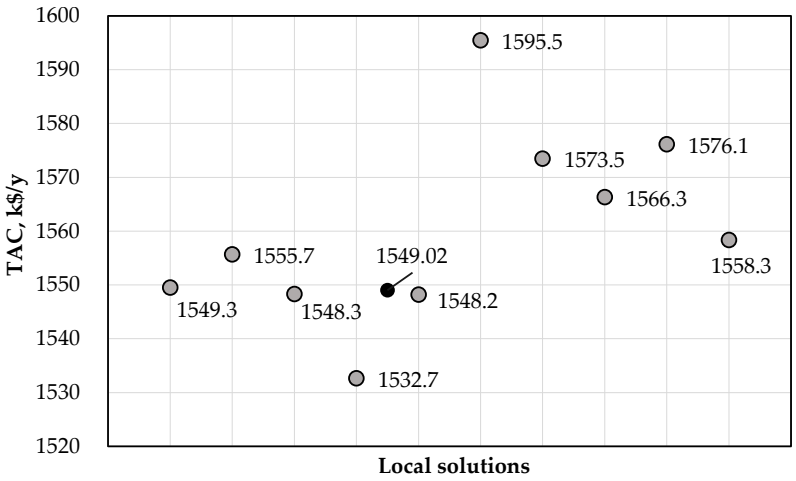

Figure 16. Local optimization solutions for Example 4.

4.5. Model Statistics

The model is solved on a computer with a 2.8 GHz processor with 4 cores and 16 GB of RAM. Table 15 shows the basic model statistics, including the model sizes and computational times for both steps of the proposed solution strategy. Statistics are presented for several cases to give a basic understanding of the model sizes and computational effort. The statistics for Example 1 are given for the model with the cost equation from Seider et al. [41] and those for Example 3 for the model with the cost equation from Towler and Sinnott [45]. The model statistics for Example 2 are given for an annualization factor of 0.1.

Table 15. Model statistics for studied examples.

	Example 1	Example 2	Example 3	Example 4
Step 1—NLP				
No. of equations	120	157	210	229
No. of continuous variables	114	153	202	221
CPU time, s	3.8	24	0.1	37.9
Step 2—MINLP				
No. of equations	353	486	773	713
No. of continuous variables	323	466	866	744
No. of discrete variables	23	31	50	45
CPU time, s	3.3	26.9	546	221

5. Conclusions

This work presents a mathematical programming approach for the simultaneous synthesis of work and heat exchange networks (WHENs). A new superstructure for work and heat integration is developed based on feasible thermodynamic paths, enabling the heating, cooling and pressure changes of defined process streams. An additional superstructure enables the HEN design of the overall problem. The proposed approach solves the optimization problem in two steps. The first step identifies hot and cold streams within the network and provides an initial solution for the second step of the proposed approach. In the second step, the WHEN is synthesized, minimizing the TAC of the network. The TAC of the network includes the OPEX (heating, cooling and electricity) and CAPEX (expanders, compressors and heat exchangers). To validate the methodology, four

examples are studied, including additional analyses of the effects of the electricity cost, equipment cost and annualization factor on the network design. By varying the equipment depreciation periods, one can obtain and compare different designs concerning the network complexity, utility consumption and required CAPEX and OPEX. One important limitation of the methodology presented in this paper is the assumption that all streams behave as ideal gases. Both real gases and liquids should have been considered, adding pumps as new pressure change equipment. Another limitation is that the two-step approach cannot guarantee the global optimality of the networks developed. However, as argued in the paper, a simultaneous (one-step) approach with such a rich superstructure would be prohibitive from a computational point of view. Future work should consider handling both liquids and real gases, including phase change operations. Additional equipment should be added to the superstructure, such as pumps (to handle liquid streams) and single-shaft turbine compressors (SSTCs) to enable additional work integration opportunities. In addition, multiple thermal utilities with corresponding cost models should be considered. Finally, multi-objective optimization should be explored with economic and exergetic objective functions.

Author Contributions: Conceptualization, N.I. and T.G.; methodology, N.I.; software, N.I.; validation, N.I., C.F. and T.G.; formal analysis, N.I.; writing—original draft preparation, N.I., C.F. and T.G.; writing—review and editing, N.I., C.F. and T.G.; visualization, N.I.; supervision, T.G.; project administration, T.G. All authors have read and agreed to the published version of the manuscript. All authors have read and agreed to the published version of the manuscript.

Funding: This publication is funded by the HighEFF—Centre for an Energy Efficient and Competitive Industry for the Future, an 8-year Research Centre under the FME scheme (Centre for Environment-Friendly Energy Research, 257632).

Institutional Review Board Statement: Not applicable.

Informed Consent Statement: Not applicable.

Data Availability Statement: Data are contained within the article.

Acknowledgments: The authors gratefully acknowledge the financial support of the Research Council of Norway and user partners of HighEFF.

Conflicts of Interest: The authors declare no conflicts of interest. The funders had no role in the design of the study; in the collection, analyses, or interpretation of data; in the writing of the manuscript; or in the decision to publish the results.

Abbreviations

CAPEX	Capital Expenditures
COMP	Compressor
EMAT	Exchanger Minimum Approach Temperature
EXP	Expander
GAMS	General Algebraic Modeling System
GDP	Generalised Disjunctive Programming
HE	Heat Exchanger
HEN	Heat Exchanger Network
HRAT	Heat Recovery Approach Temperature
MINLP	Mixed Integer Nonlinear Programming
MP	Mathematical Programming
NLP	Nonlinear Programming
OPEX	Operational Expenditures
PA	Pinch Analysis
STHE	Shell and Tube Heat Exchangers
TAC	Total Annualized Cost
WHI	Work and Heat Integration
WHEN	Work and Heat Exchange Network

Indices

i	Hot stream
j	Cold stream
k	Pressure change stage
s	Process stream

Sets

K	Pressure change stages
S	Process streams

Subscripts/Superscripts

bypass	Bypass
C	Cooler
comp	Compressor
cons	Consumed
cs	Cold stream/Cold supply
ct	Cold target
CU	Cold utility
ehs	Exchanger's hot stream
ecs	Exchanger's cold stream
exc	Exchanger
exp	Expander
H	Heater
hs	Hot stream/Hot supply
ht	Hot target
HU	Hot utility
IC	Inter-stage cooling
id	Ideal
IH	Inter-stage heating
in	Inlet
m	Mixer
max	Maximum
out	Outlet
prod	Produced
ub	Upper bound
valve	Expansion valve

Parameters

a	Fixed cost for equipment, \$
af	Equipment investment annualization factor, 1/y
b	Variable cost coefficient for equipment, \$/attribute
BINT	Binary parameter denoting existence of bypass, $[-]$
C_{CU}	Cold utility cost, \$/kWy
C_{HU}	Hot utility cost, \$/kWy
C_{el}	Electricity cost, \$/kWy
CINT	Binary parameter denoting existence of compression stages, $[-]$
dp	Depreciation period for investment, y
EINT	Binary parameter denoting existence of expansion stages, $[-]$
FBM	Bare module factor, $[-]$
h	Individual heat transfer coefficient, kW/(m^{2}K)
ir	Interest rate for investment, %/100
n	Cost exponent for equipment
κ	Isentropic expansion/compression coefficient, $[-]$
μ	Joule–Thompson expansion coefficient, K/MPa
η	Isentropic efficiency of compressor/expander, $[-]$
$T_s^{(in)}$	Process stream s supply temperature, K
$T_s^{(\mathrm{out})}$	Process stream s target temperature, K
$p_s^{(in)}$	Process stream s supply pressure, MPa
$p_s^{(\mathrm{out})}$	Process stream s target pressure, MPa

Γ	Upper bound for temperature driving force, K
Continuous variables	
A	Heat exchange area, m^2
m, f	Heat capacity flow rate, kW/K
T	Temperature, K
p	Pressure, MPa
q	Heat load, kW
ΔTh	Temperature difference at hot end of heat exchanger, K
ΔTc	Temperature difference at cold end of heat exchanger, K
Binary variables	
z	Existence of equipment, -

Appendix A

Appendix A.1. Identification of Streams

The identification and ordering of hot and cold streams has been done according to the proposed WHI superstructure. To facilitate the understanding of the stream numbering, an extended superstructure for two process streams ($|S| = 2$) and three pressure change stages ($|K| = 3$) is shown in Figure A1. The numbering of the streams starts from the hot and cold streams related to the initial stream splitters for hot (HSS_s) and cold streams (CSS_s). The number of related hot/cold streams equals the number of streams s ($i = s$) and the connecting relations between the heat capacity flow rates and inlet/outlet temperatures are given by Equations (A1)–(A6).

$$f_i = m_s^{(\mathrm{hs})}, \quad i = s \tag{A1}$$

$$T_i^{(\mathrm{in})} = T_s^{(\mathrm{in})}, \quad i = s \tag{A2}$$

$$T_i^{(\mathrm{out})} = T_s^{(\mathrm{hs,out})}, \quad i = s \tag{A3}$$

$$f_j = m_s^{(\mathrm{cs})}, \quad j = s \tag{A4}$$

$$T_j^{(\mathrm{in})} = T_s^{(\mathrm{in})}, \quad j = s \tag{A5}$$

$$T_j^{(\mathrm{out})} = T_s^{(\mathrm{cs,out})}, \quad j = s \tag{A6}$$

The numbering of the streams continues with the hot/cold streams related to the hot target (HTM_s) and cold target (CTM_s) stream mixers. The number of related streams equals the number of streams s. However, the numbering starts from $|S|$, as given by Equations (A7)–(A12).

$$f_i = m_s^{(\mathrm{ht})}, \quad i = s + |S| \tag{A7}$$

$$T_i^{(\mathrm{in})} = T_s^{(\mathrm{ht,in})}, \quad i = s + |S| \tag{A8}$$

$$T_i^{(\mathrm{out})} = T_s^{(\mathrm{out})}, \quad i = s + |S| \tag{A9}$$

$$f_j = m_s^{(\mathrm{ct})}, \quad j = s + |S| \tag{A10}$$

$$T_j^{(\mathrm{in})} = T_s^{(\mathrm{ct,in})}, \quad j = s + |S| \tag{A11}$$

$$T_j^{(\mathrm{out})} = T_s^{(\mathrm{out})}, \quad j = s + |S| \tag{A12}$$

Cooling the streams before compression reduces work consumption. At the same time, compression increases the temperature of the stream. As a result, streams leaving the compression stages are defined as hot streams requiring inter-stage cooling. The numbering of hot streams continues from $2|S|$, and the number of hot streams is related to the number of compression stages $|K| - 1$, as described by the connecting Equations (A13)–(A15).

$$f_i = m_s^{(\mathrm{comp})}, \quad i = 2|S| + s(|K| - 1) - (|K| - 1 - k) \wedge k < |K| \wedge |K| > 1 \tag{A13}$$

$$T_i^{(\text{in})} = T_{s,k}^{(\text{IC,in})}, \quad i = 2|S| + s(|K|-1) - (|K|-1-k) \wedge k < |K| \wedge |K| > 1 \tag{A14}$$

$$T_i^{(\text{out})} = T_{s,k}^{(\text{IC,out})}, \quad i = 2|S| + s(|K|-1) - (|K|-1-k) \wedge k < |K| \wedge |K| > 1 \tag{A15}$$

Heating of the streams before expansion increases the work production. At the same time, expansion decreases the temperature of the stream. As a result, streams leaving the expansion stages are defined as cold streams requiring inter-stage heating. The numbering of the cold streams continues from $2|S|$, and the number of cold streams is related to the number of expansion stages $|K|-1$, as described by the connecting Equations (A16)–(A18).

$$f_j = m_s^{(\text{exp})}, \quad j = 2|S| + s(|K|-1) - (|K|-1-k) \wedge k < |K| \wedge |K| > 1 \tag{A16}$$

$$T_j^{(\text{in})} = T_{s,k}^{(\text{IH,in})}, \quad j = 2|S| + s(|K|-1) - (|K|-1-k) \wedge k < |K| \wedge |K| > 1 \tag{A17}$$

$$T_j^{(\text{out})} = T_{s,k}^{(\text{IH,out})}, \quad j = 2|S| + s(|K|-1) - (|K|-1-k) \wedge k < |K| \wedge |K| > 1 \tag{A18}$$

Appendix A.2. Additional Constraints

To facilitate the solution of the second MINLP model, the binary variables identifying the existence of heat exchangers, heaters and coolers are constrained to values 0 or 1 based on the existence of hot and cold streams within the first NLP model as follows:

$$z_{i,j} \leq \begin{cases} 1 & \text{if } ec_i > 0 \wedge ec_j > 0 \\ 0 & \text{else} \end{cases} \tag{A19}$$

$$z_i \leq \begin{cases} 1 & \text{if } ec_i > 0 \\ 0 & \text{else} \end{cases} \tag{A20}$$

$$z_j \leq \begin{cases} 1 & \text{if } ec_j > 0 \\ 0 & \text{else} \end{cases} \tag{A21}$$

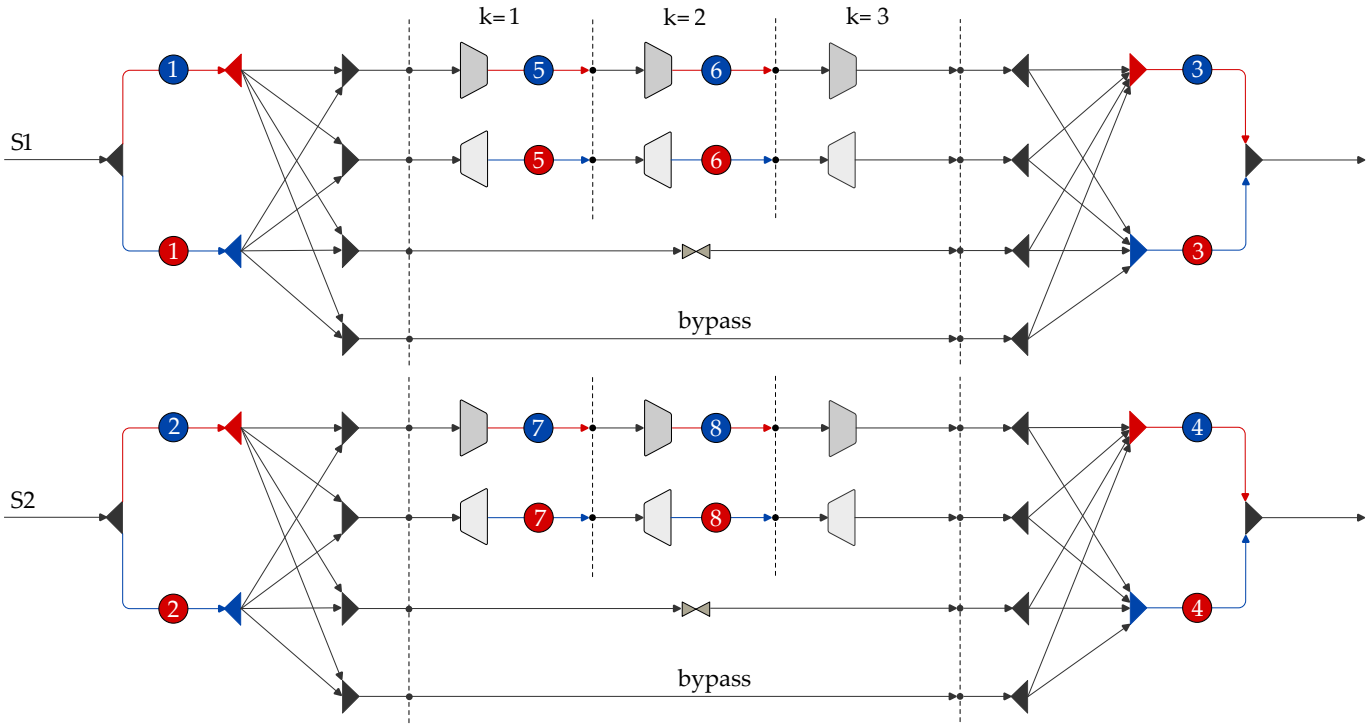

Figure A1. Representative WHI superstructure for two process streams and three pressure change stages.

References

1. Klemeš, J.J.; Kravanja, Z. Forty years of Heat Integration: Pinch Analysis (PA) and Mathematical Programming (MP). *Curr. Opin. Chem. Eng.* **2013**, *2*, 461–474. https://doi.org/10.1016/J.COCHE.2013.10.003.
2. Fu, C.; Vikse, M.; Gundersen, T. Work and heat integration: An emerging research area. *Energy* **2018**, *158*, 796–806. https://doi.org/10.1016/j.energy.2018.06.030.
3. Aspelund, A.; Berstad, D.O.; Gundersen, T. An Extended Pinch Analysis and Design procedure utilizing pressure based exergy for subambient cooling. *Appl. Therm. Eng.* **2007**, *27*, 2633–2649. https://doi.org/10.1016/j.applthermaleng.2007.04.017.
4. Fu, C.; Gundersen, T. Integrating compressors into heat exchanger networks above ambient temperature. *AIChE J.* **2015**, *61*, 3770–3785. https://doi.org/10.1002/aic.15045.
5. Fu, C.; Gundersen, T. Integrating expanders into heat exchanger networks above ambient temperature. *AIChE J.* **2015**, *61*, 3404–3422. https://doi.org/10.1002/aic.14968.
6. Fu, C.; Wang, X.; Gundersen, T. The importance of thermodynamic insight in Work and Heat Exchange Network Design. *Chem. Eng. Trans.* **2020**, *81*, 127–132. https://doi.org/10.3303/CET2081022.
7. Wechsung, A.; Aspelund, A.; Gundersen, T.; Barton, P.I. Synthesis of heat exchanger networks at subambient conditions with compression and expansion of process streams. *AIChE J.* **2011**, *57*, 2090–2108. https://doi.org/10.1002/aic.12412.
8. Huang, K.; Karimi, I.A. Work-heat exchanger network synthesis (WHENS). *Energy* **2016**, *113*, 1006–1017. https://doi.org/10.1016/j.energy.2016.07.124.
9. Huang, K.F.; Al-mutairi, E.M.; Karimi, I.A. Heat exchanger network synthesis using a stagewise superstructure with non-isothermal mixing. *Chem. Eng. Sci.* **2012**, *73*, 30–43. https://doi.org/10.1016/j.ces.2012.01.032.
10. Onishi, V.C.; Ravagnani, M.A.; Caballero, J.A. Simultaneous synthesis of work exchange networks with heat integration. *Chem. Eng. Sci.* **2014**, *112*, 87–107. https://doi.org/10.1016/j.ces.2014.03.018.
11. Yee, T.F.; Grossmann, I.E. Simultaneous optimization models for heat integration—II. Heat exchanger network synthesis. *Comput. Chem. Eng.* **1990**, *14*, 1165–1184. https://doi.org/10.1016/0098-1354(90)85010-8.
12. Onishi, V.C.; Ravagnani, M.A.; Caballero, J.A. MINLP Model for the Synthesis of Heat Exchanger Networks with Handling Pressure of Process Streams. *Comput. Aided Chem. Eng.* **2014**, *33*, 163–168. https://doi.org/10.1016/B978-0-444-63456-6.50028-4.
13. Pavão, L.V.; Costa, C.B.; Ravagnani, M.A. A new framework for work and heat exchange network synthesis and optimization. *Energy Convers. Manag.* **2019**, *183*, 617–632. https://doi.org/10.1016/j.enconman.2019.01.018.
14. Onishi, V.C.; Ravagnani, M.A.S.S.; Caballero, J.A. Simultaneous synthesis of heat exchanger networks with pressure recovery: Optimal integration between heat and work. *AIChE J.* **2014**, *60*, 893–908. https://doi.org/10.1002/aic.14314.
15. Pavão, L.V.; Costa, C.B.B.; Ravagnani, M.A.S.S. An Enhanced Stage-wise Superstructure for Heat Exchanger Networks Synthesis with New Options for Heaters and Coolers Placement. *Ind. Eng. Chem. Res.* **2018**, *57*, 2560–2573. https://doi.org/10.1021/acs.iecr.7b03336.
16. Pavão, L.V.; Caballero, J.A.; Ravagnani, M.A.; Costa, C.B. An extended method for work and heat integration considering practical operating constraints. *Energy Convers. Manag.* **2020**, *206*, 112469. https://doi.org/10.1016/j.enconman.2020.112469.
17. Nair, S.K.; Nagesh Rao, H.; Karimi, I.A. Framework for work-heat exchange network synthesis (WHENS). *AIChE J.* **2018**, *64*, 2472–2485. https://doi.org/10.1002/aic.16129.
18. Onishi, V.C.; Quirante, N.; Ravagnani, M.A.; Caballero, J.A. Optimal synthesis of work and heat exchangers networks considering unclassified process streams at sub and above-ambient conditions. *Appl. Energy* **2018**, *224*, 567–581. https://doi.org/10.1016/j.apenergy.2018.05.006.
19. Duran, M.A.; Grossmann, I.E. Simultaneous optimization and heat integration of chemical processes. *Aiche J.* **1986**, *32*, 123–138.
20. Quirante, N.; Caballero, J.A.; Grossmann, I.E. A novel disjunctive model for the simultaneous optimization and heat integration. *Comput. Chem. Eng.* **2017**, *96*, 149–168. https://doi.org/10.1016/j.compchemeng.2016.10.002.
21. Li, J.; Demirel, S.E.; Hasan, M.M.F. Building Block-Based Synthesis and Intensification of Work-Heat Exchanger Networks (WHENS). *Processes* **2019**, *7*, 23. https://doi.org/10.3390/pr7010023.
22. Pavão, L.V.; Caballero, J.A.; Ravagnani, M.A.; Costa, C.B. A pinch-based method for defining pressure manipulation routes in work and heat exchange networks. *Renew. Sustain. Energy Rev.* **2020**, *131*, 109989. https://doi.org/10.1016/j.rser.2020.109989.
23. Linnhoff, B.; Ahmad, S. Cost optimum heat exchanger networks—1. Minimum energy and capital using simple models for capital cost. *Comput. Chem. Eng.* **1990**, *14*, 729–750. https://doi.org/10.1016/0098-1354(90)87083-2.
24. Yu, H.; Vikse, M.; Anantharaman, R.; Gundersen, T. Model reformulations for Work and Heat Exchange Network (WHEN) synthesis problems. *Comput. Chem. Eng.* **2019**, *125*, 89–97. https://doi.org/10.1016/j.compchemeng.2019.02.018.
25. Lin, Q.; Liao, Z.; Sun, J.; Jiang, B.; Wang, J.; Yang, Y. Targeting and Design of Work and Heat Exchange Networks. *Ind. Eng. Chem. Res.* **2020**, *59*, 12471–12486. https://doi.org/10.1021/acs.iecr.0c00308.
26. Lin, Q.; Chang, C.; Liao, Z.; Sun, J.; Jiang, B.; Wang, J.; Yang, Y. Efficient Strategy for the Synthesis of Work and Heat Exchange Networks. *Ind. Eng. Chem. Res.* **2021**, *60*, 1756–1773. https://doi.org/10.1021/acs.iecr.0c05460.
27. Lin, Q.; Liao, Z.; Bagajewicz, M.J. Globally optimal design of Minimal WHEN systems using enumeration. *AIChE J.* **2023**, *69*, e17878. https://doi.org/10.1002/aic.17878.
28. Yang, R.; Zhuang, Y.; Zhang, L.; Du, J.; Shen, S. A thermo-economic multi-objective optimization model for simultaneous synthesis of heat exchanger networks including compressors. *Chem. Eng. Res. Des.* **2020**, *153*, 120–135. https://doi.org/10.1016/j.cherd.2019.10.011.

29. Zhuang, Y.; Yang, R.; Zhang, L.; Du, J.; Shen, S. Simultaneous synthesis of sub and above-ambient heat exchanger networks including expansion process based on an enhanced superstructure model. *Chin. J. Chem. Eng.* **2020**, *28*, 1344–1356. https://doi.org/10.1016/j.cjche.2020.02.026.
30. Zhuang, Y.; Xing, Y.; Zhang, L.; Liu, L.; Du, J.; Shen, S. An enhanced superstructure-based model for work-integrated heat exchange network considering inter-stage multiple utilities optimization. *Comput. Chem. Eng.* **2021**, *152*, 107388. https://doi.org/10.1016/j.compchemeng.2021.107388.
31. Braccia, L.; Luppi, P.; Vallarella, A.J.; Zumoffen, D. Generalized simultaneous optimization model for synthesis of heat and work exchange networks. *Comput. Chem. Eng.* **2022**, *168*, 108036. https://doi.org/10.1016/j.compchemeng.2022.108036.
32. Yu, H.; Fu, C.; Gundersen, T. Work Exchange Networks (WENs) and Work and Heat Exchange Networks (WHENs): A Review of the Current State of the Art. *Ind. Eng. Chem. Res.* **2020**, *59*, 507–525. https://doi.org/10.1021/acs.iecr.9b04932.
33. Floudas, C.A.; Ciric, A.R.; Grossmann, I.E. Automatic synthesis of optimum heat exchanger network configurations. *AIChE J.* **1986**, *32*, 276–290. https://doi.org/10.1002/aic.690320215.
34. Yu, H.; Fu, C.; Vikse, M.; He, C.; Gundersen, T. Identifying optimal thermodynamic paths in work and heat exchange network synthesis. *AIChE J.* **2019**, *65*, 549–561. https://doi.org/10.1002/aic.16437.
35. Biegler, L.T.; Grossmann, I.E.; Westerberg, A.W. *Systematic Methods for Chemical Process Design*; Prentice Hall, Inc., NJ, USA, 1997.
36. Chen, J. Comments on improvements on a replacement for the logarithmic mean. *Chem. Eng. Sci.* **1987**, *42*, 2488–2489. https://doi.org/10.1016/0009-2509(87)80128-8.
37. Chen, J. Logarithmic mean: Chen's approximation or explicit solution? *Comput. Chem. Eng.* **2019**, *120*, 1–3. https://doi.org/10.1016/j.compchemeng.2018.10.002.
38. Smith, R. *Chemical Process Design and Integration*, 2nd ed.; John Wiley & Sons, Inc.: Chichester, West Sussex, UK, 2016.
39. GAMS Development Corporation. *General Algebraic Modeling System (GAMS)*: Release 36.1.0; Fairfax, VA, USA, 2022.
40. Systat Software Inc. *SigmaPlot v 14*; San Jose, CA, USA, 2017.
41. Seider, W.; Seader, J.; Lewin, D. *Product and Process Design Principles: Synthesis, Analysis and Evaluation*, 3rd ed.; John Wiley & Sons, Inc.: Hoboken, NJ, USA, 2008.
42. Peters, M.; Timmerhaus, K.; West, R. *Plant Design and Economics for Chemical Engineers, 4th ed.*; McGraw-Hill Chemical Engineering Series; McGraw-Hill, Inc.: New York, NY, USA, 2003.
43. Couper, J.R.; Penney, W.R.; Fair, J.R.; Walas, S.M. 21—Costs of Individual Equipment. In *Chemical Process Equipment*, 3rd ed.; Couper, J.R., Penney, W.R., Fair, J.R., Walas, S.M., Eds.; Butterworth-Heinemann: Boston, MA, USA, 2012; pp. 731–741. https://doi.org/10.1016/B978-0-12-396959-0.00021-5.
44. Woods, D.R., Appendix D: Capital Cost Guidelines. In *Rules of Thumb in Engineering Practice*; Wiley-VCH Verlag GmbH & Co.: KGaA, Weinheim, Germany, 2007; pp. 376–436. https://doi.org/10.1002/9783527611119.app4.
45. Towler, G.; Sinnott, R. Chapter 7—Capital cost estimating. In *Chemical Engineering Design*, 3rd ed.; Towler, G., Sinnott, R., Eds.; Butterworth-Heinemann: Cambridge, MA, USA, 2022; pp. 239–278. https://doi.org/10.1016/B978-0-12-821179-3.00007-8.
46. Turton, R.; Bailie, R.C.; Whiting, W.B.; Shaeiwitz, J.A.; Bhattacharyya, D.: *Analysis, Synthesis, and Design of Chemical Processes*; Prentice-Hall International Series in Engineering; Prentice Hall: Upper Saddle River, NJ, USA, 2012.
47. Shah, N.M.; Rangaiah, G.P.; Hoadley, A.F. Multi-objective optimization of multi-stage gas-phase refrigeration systems. In *Multi-Objective Optimization: Techniques and Application in Chemical Engineering*; World Scientific Publishing Co. Pte. Ltd.: Singapore, 2017; pp. 247–290.
48. Fu, C.; Gundersen, T. Correct integration of compressors and expanders in above ambient heat exchanger networks. *Energy* **2016**, *116*, 1282–1293. https://doi.org/10.1016/j.energy.2016.05.092.